[redacted]

Copy 81
RM L50K24

NACA

RESEARCH MEMORANDUM

CLASSIFICATION CHANGED TO Unclassified
BY AUTHORITY OF NASA Bull. #128
ON 1/17/67 OF JK

SOME RECENT DATA FROM FLIGHT TESTS OF ROCKET-POWERED MODELS

By Langley Pilotless Aircraft Research Division

Langley Aeronautical Laboratory
Langley Field, Va.

NATIONAL ADVISORY COMMITTEE FOR AERONAUTICS

WASHINGTON

February 7, 1951

[redacted]

 [redacted]

NATIONAL ADVISORY COMMITTEE FOR AERONAUTICS

RESEARCH MEMORANDUM

SOME RECENT DATA FROM FLIGHT TESTS OF ROCKET-POWERED MODELS

By Langley Pilotless Aircraft Research Division

A survey has been made of recent flight data from rocket-powered models which are thought to be particularly applicable to the current U. S. Air Force interceptor competition and which are not yet available in the usual report form. These data are presented herein along with some recently published data which are directly applicable. The data are presented with no discussion or analysis. Some of the data have been taken from investigations that are still incomplete. Proper analysis and discussion will be made in forthcoming NACA papers.

The attached table presents a listing of the subjects covered, the configurations for which data are presented, and references to the figures containing model drawings and data for each configuration.

Langley Aeronautical Laboratory
National Advisory Committee for Aeronautics
Langley Air Force Base, Va.

[redacted]

REFERENCES

1. Schult, Eugene D.: Comparison of Large-Scale Flight Measurements of Zero-Lift Drag at Mach Numbers from 0.9 to 1.7 of Two Wing-Body Combinations Having Similar 60° Triangular Wings with NACA 65A003 Sections. NACA RM L50I22, 1950.

2. Katz, Ellis: Flight Investigations from High Subsonic to Supersonic Speeds to Determine the Zero-Lift Drag of a Transonic Research Vehicle Having Wings of 45° Sweepback, Aspect Ratio 4, Taper Ratio 0.6, and NACA 65A006 Airfoil Sections. NACA RM L9H30, 1949.

3. Mitcham, Grady L., Stevens, Joseph E., and Norris, Harry P.: Aerodynamic Characteristics and Flying Qualities of a Tailless Triangular-Wing Airplane Configuration As Obtained from Flights of Rocket-Propelled Models at Transonic and Low Supersonic Speeds. NACA RM L9L07, 1950.

4. Niewald, Roy J., and Moul, Martin T.: The Longitudinal Stability, Control Effectiveness, and Control Hinge-Moment Characteristics Obtained from a Flight Investigation of a Canard Missile Configuration at Transonic and Supersonic Speeds. NACA RM L50I27, 1950.

5. Mitcham, Grady L., and Blanchard, Willard S., Jr.: Summary of the Aerodynamic Characteristics and Flying Qualities Obtained from Flights of Rocket-Propelled Models of an Airplane Configuration Incorporating a Sweptback Inversely Tapered Wing at Transonic and Low-Supersonic Speeds. NACA RM L50G18a, 1950.

6. Gillis, Clarence L., Peck, Robert F., and Vitale, A. James: Preliminary Results from a Free-Flight Investigation at Transonic and Supersonic Speeds of the Longitudinal Stability and Control Characteristics of an Airplane Configuration with a Thin Straight Wing of Aspect Ratio 3. NACA RM L9K25a, 1950.

7. Gillis, Clarence L.: Buffeting Information Obtained from Rocket-Propelled Airplane Models Having Thin Unswept Wings. NACA RM L50H22a, 1950.

8. D'Aiutolo, Charles T., and Mason, Homer P.: Preliminary Results of the Flight Investigation between Mach Numbers of 0.80 and 1.36 of a Rocket-Powered Model of a Supersonic Airplane Configuration Having a Tapered Wing with Circular-Arc Sections and 40° Sweepback. NACA RM L50H29a, 1950.

9. Hart, Roger G.: Flight Investigation at Mach Numbers from 0.8 to 1.5 to Determine the Effects of Nose Bluntness on the Total-Drag of Two Fin-Stabilized Bodies of Revolution. NACA RM L50I08a, 1950.

10. Baals, Donald D., Smith, Norman F., and Wright, John B.: The Development and Application of High-Critical-Speed Nose Inlets. NACA Rep. 920, 1948.

11. Edmondson, James L., and Sanders, E. Claude, Jr.: A Free-Flight Technique for Measuring Damping in Roll by Use of Rocket-Powered Models and Some Initial Results for Rectangular Wings. NACA RM L9I01, 1949.

TABLE

Item	Model	Figure numbers	
		Configurations	Data
Wing drag:			
(1) Zero-lift drag (Reynolds No. .10 to 50 × 10^6)			
(a) 3, 4, and 6-percent-thick delta wings	1, 5, 6, 7	1, 3	2, 4, 8, 9, 10
(b) 6-percent-thick 45° swept wing (two different bodies)	3, 4	3	4, 6, 7
(c) 4.5-percent-thick straight wing	2	3	4, 5
(2) Drag due to lift			
(a) 6.5-percent-thick delta trimmed with elevator	8	11	17
(b) 6.5-percent-thick delta trimmed with canard surfaces	9	12	17
(c) 40° and 60° swept wings	10, 11	13, 14	18, 19
(d) 4.5-percent-thick straight wings	12	15	19
Body drag:			
(1) Drag of radome noses	13	20	20
(2) Drag of canopies	14	21	22
Inlet drag and pressure recovery:			
(1) Sharpened-lip nose inlet and basic body	15, 16	23	24, 25
(2) Subsonic nose inlet and basic body	15, 17	23	26, 27
Lift characteristics:			
(1) 6.5-percent-thick delta wings, tailless and with canard	8, 9	11, 12	28
(2) 40°, 42°, and 60° swept wings with tail	10, 11, 18	13, 14, 16	28
(3) 4.5-percent-thick straight wing with tail	12	15	28
Aerodynamic-center location:			
(1) 6.5-percent-thick delta wings, tailless and with canard	8, 9	11, 12	29
(2) 40°, 42°, and 60° swept wings with tail	10, 11, 18	13, 14, 16	29
(3) 4.5-percent-thick straight wing with tail	12	15	29
Longitudinal control:			
(1) 6.5-percent-thick delta wings with elevator (tailless) and with canard	8, 9	11, 12	30
(2) 40° swept wing with elevator	10	13	30
(3) 4.5-percent-thick straight wing with all-movable tail	12	15	30
Longitudinal damping:			
(1) 6.5-percent-thick delta wings, tailless and with canard	8, 9	11, 12	31
(2) 40°, 42°, and 60° swept wings with tail	10, 11, 18	13, 14, 16	31
(3) 4.5-percent-thick straight wing with tail	12	15	31
Damping in roll:			
(1) 6-percent-thick 45°, 60°, and 70° delta wings	19	32, 33	33
(2) 35°, 40°, 45°, and 63° swept wings	20, 21, 22, 23, 24	32, 34, 35, 36	34, 35, 36
(3) 4.5 and 6-percent-thick straight wings	25, 26	37	37

NACA

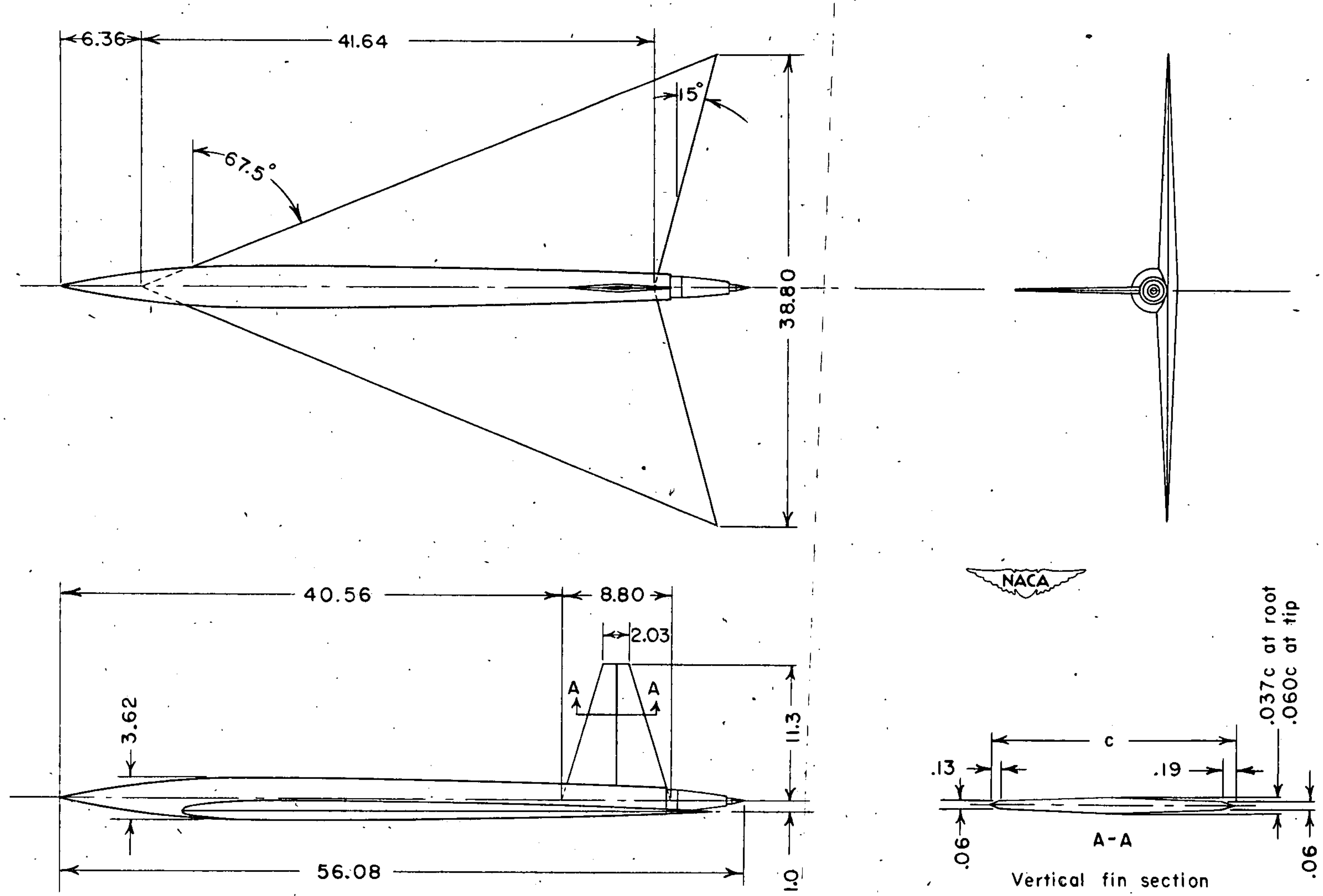

(a) Arrow wing-body combination; 4-percent-thick wing.

Figure 1.- General arrangement of model 1. All dimensions are in inches.

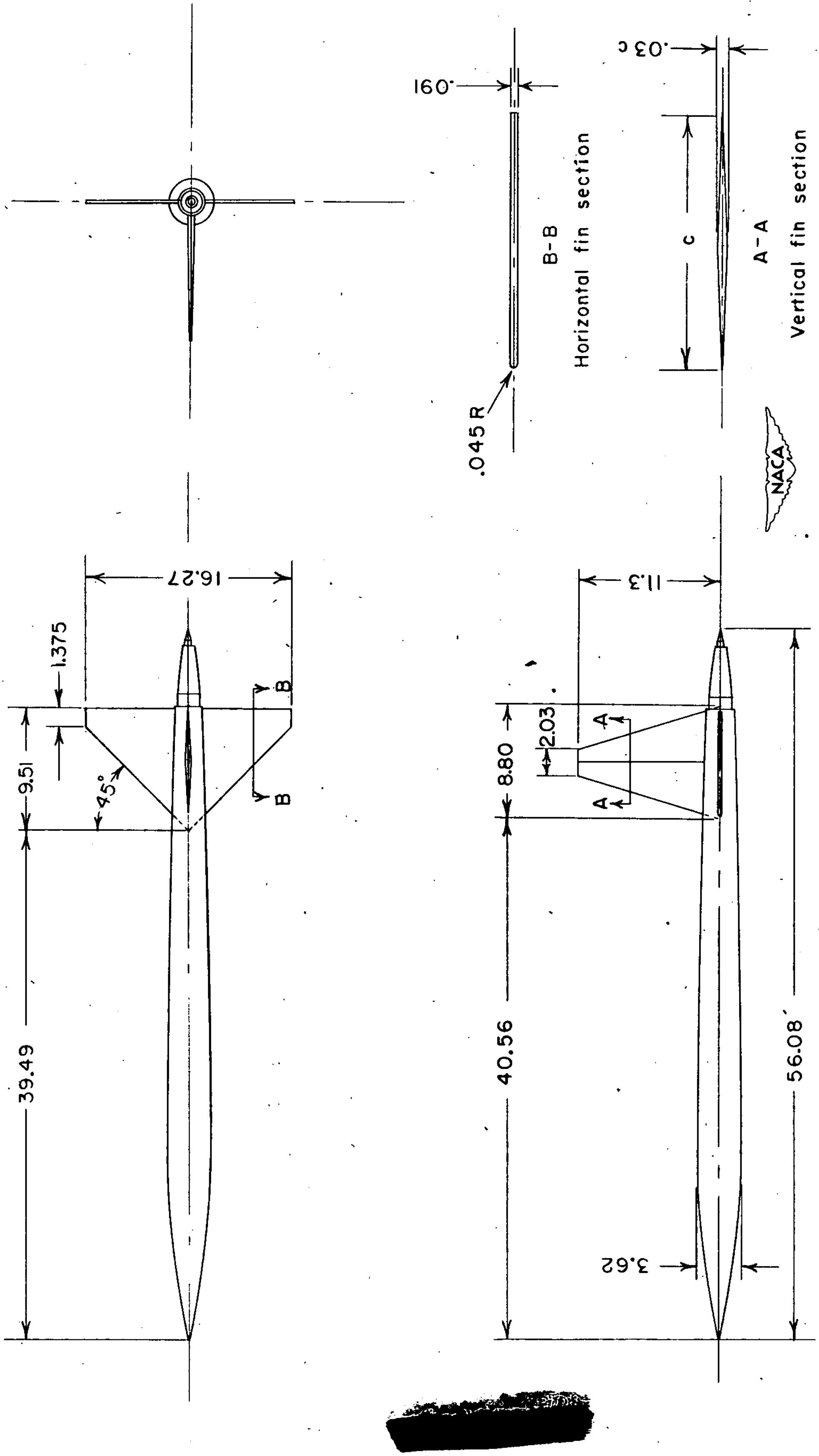

(b) Wingless model.

Figure 1.- Concluded.

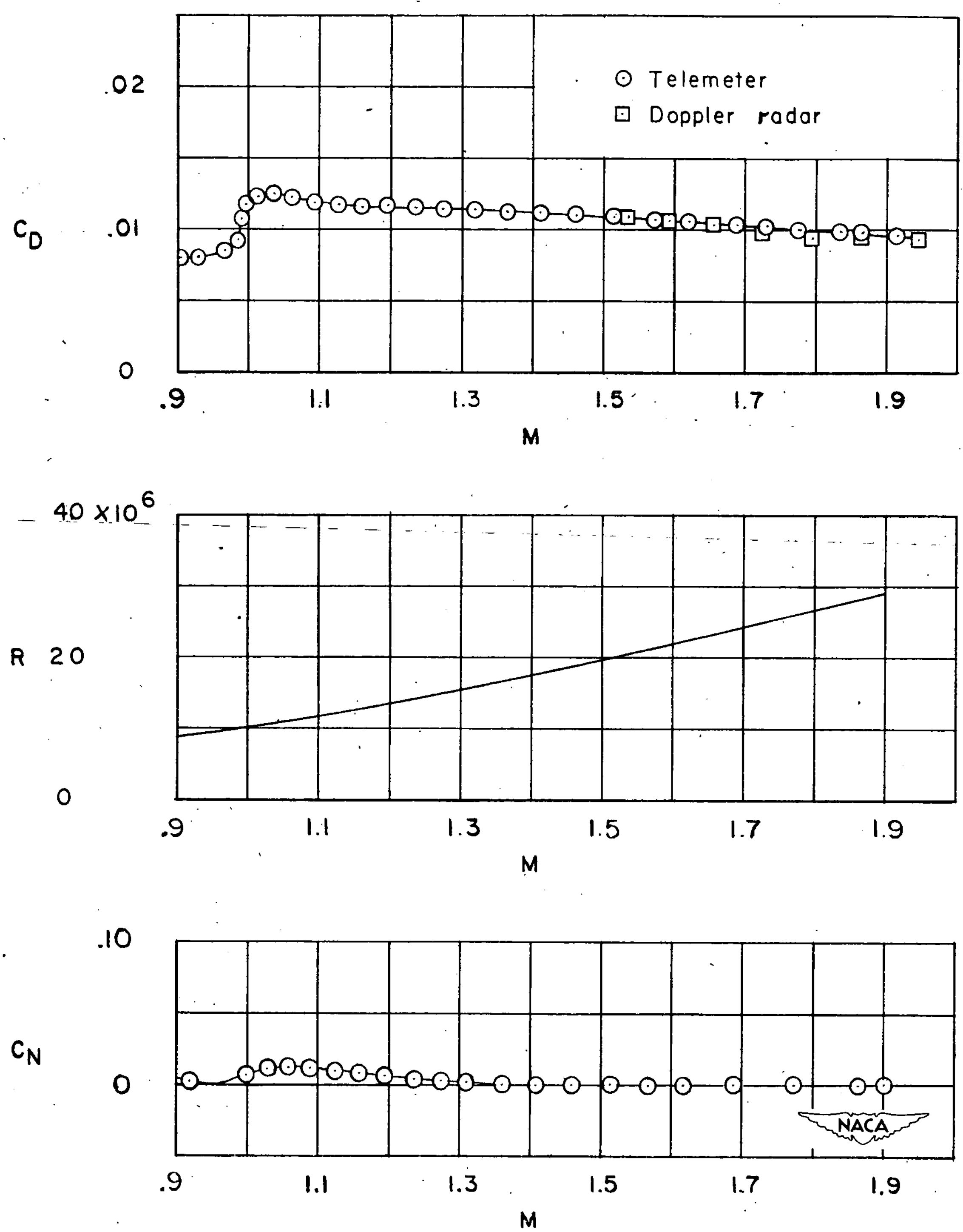

(a) C_D, R, and C_N against M for arrow wing-body model.

Figure 2.- Data from coasting flight of model 1. C_D based on total wing to fuselage center line.

[redacted]

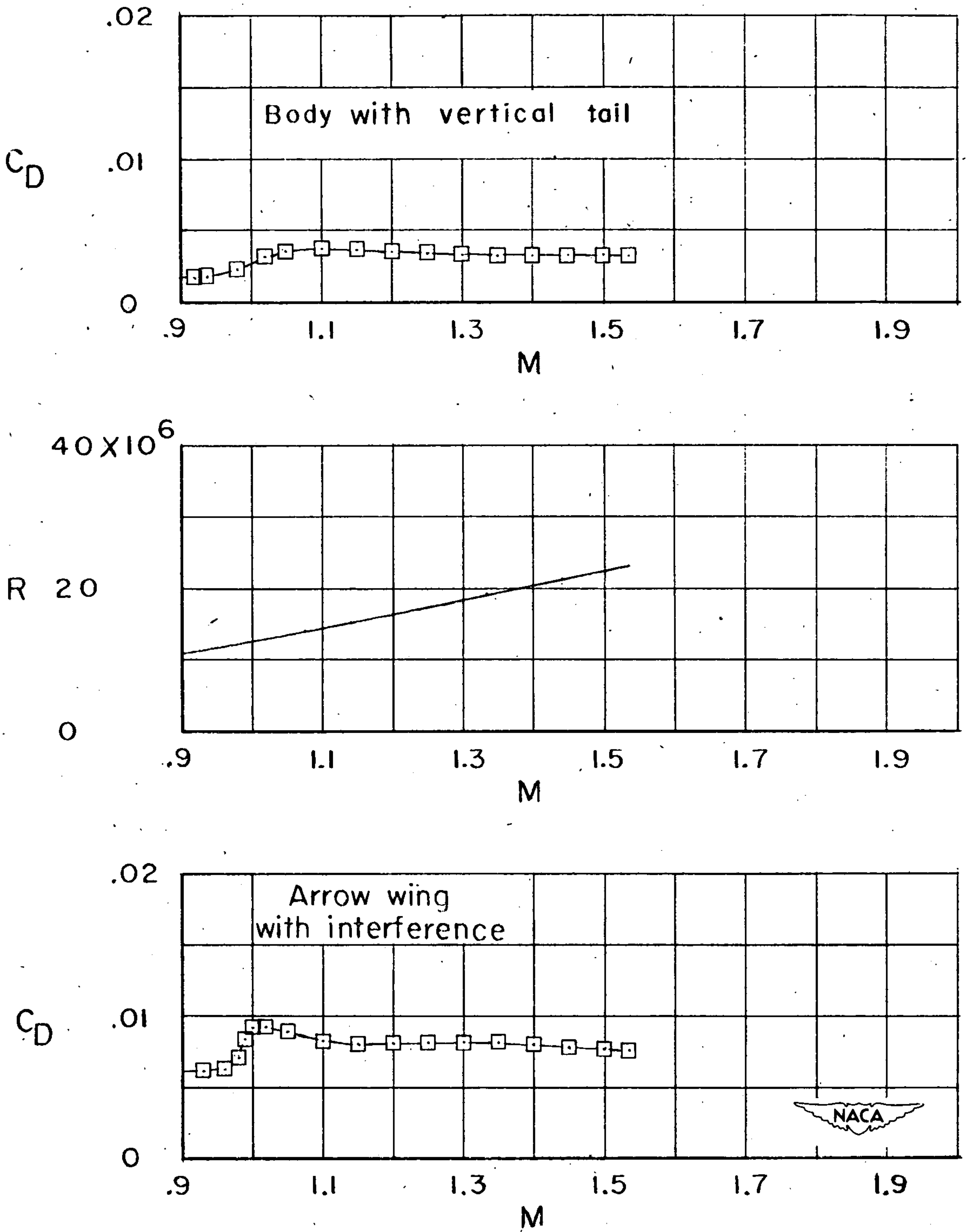

(b) C_D and R against M from wingless model.

Figure 2.- Concluded.

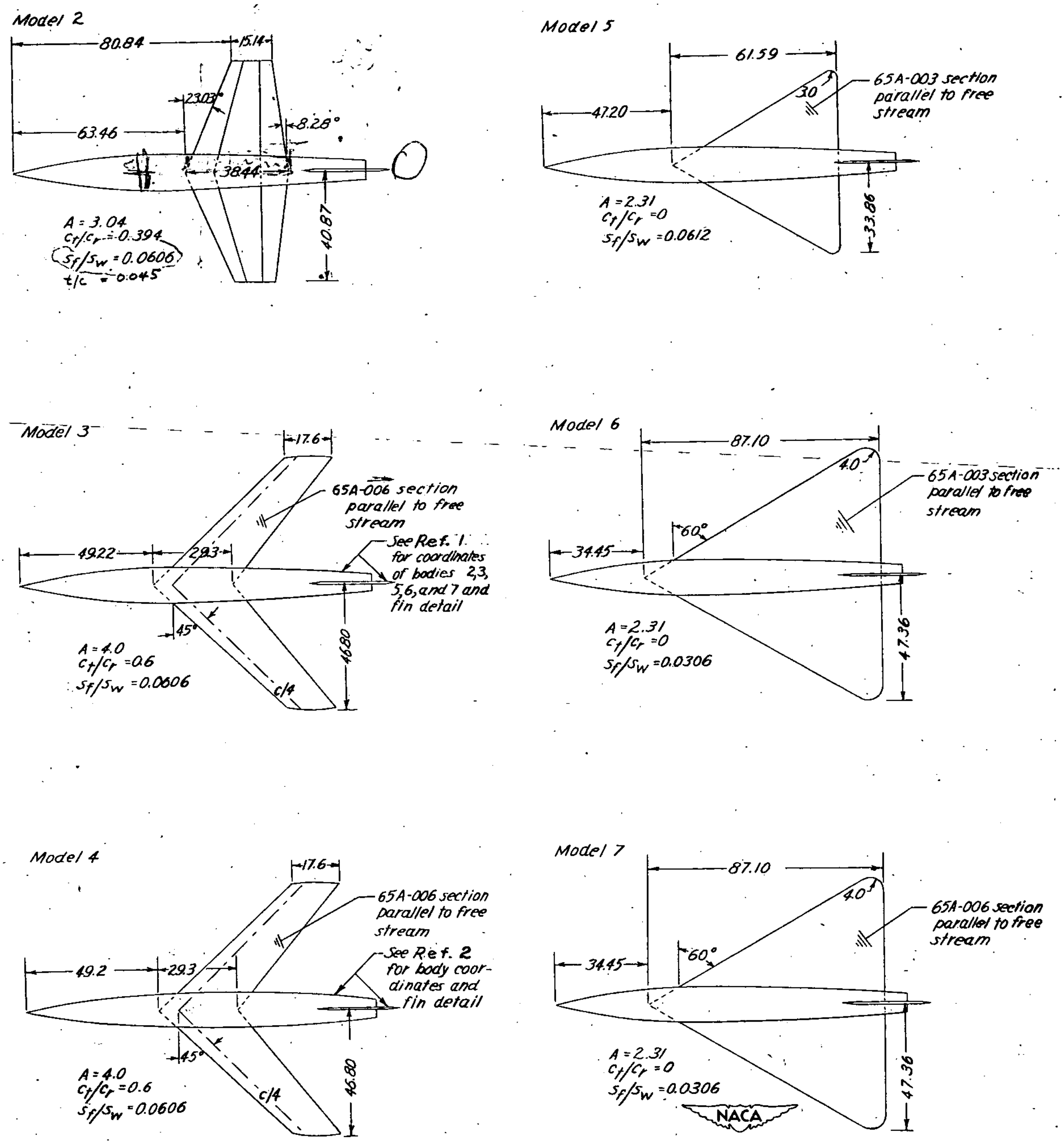

Figure 3.- Plan forms of models 2, 3, 4, 5, 6, and 7. (All dimensions are in inches.)

[redacted]

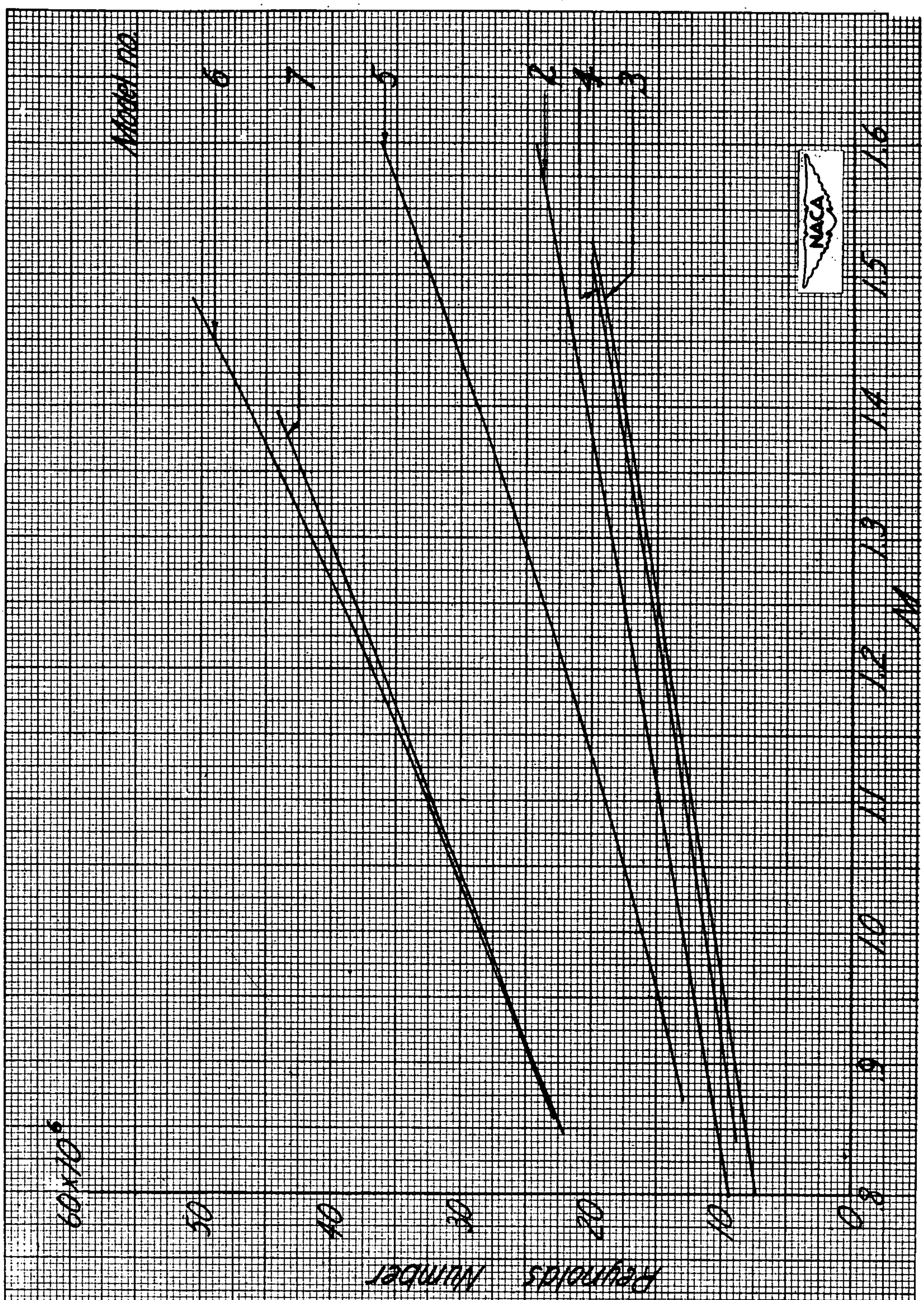

Figure 4.- Variation of Reynolds number with Mach number for the wing-body configuration, based on wing mean aerodynamic chord.

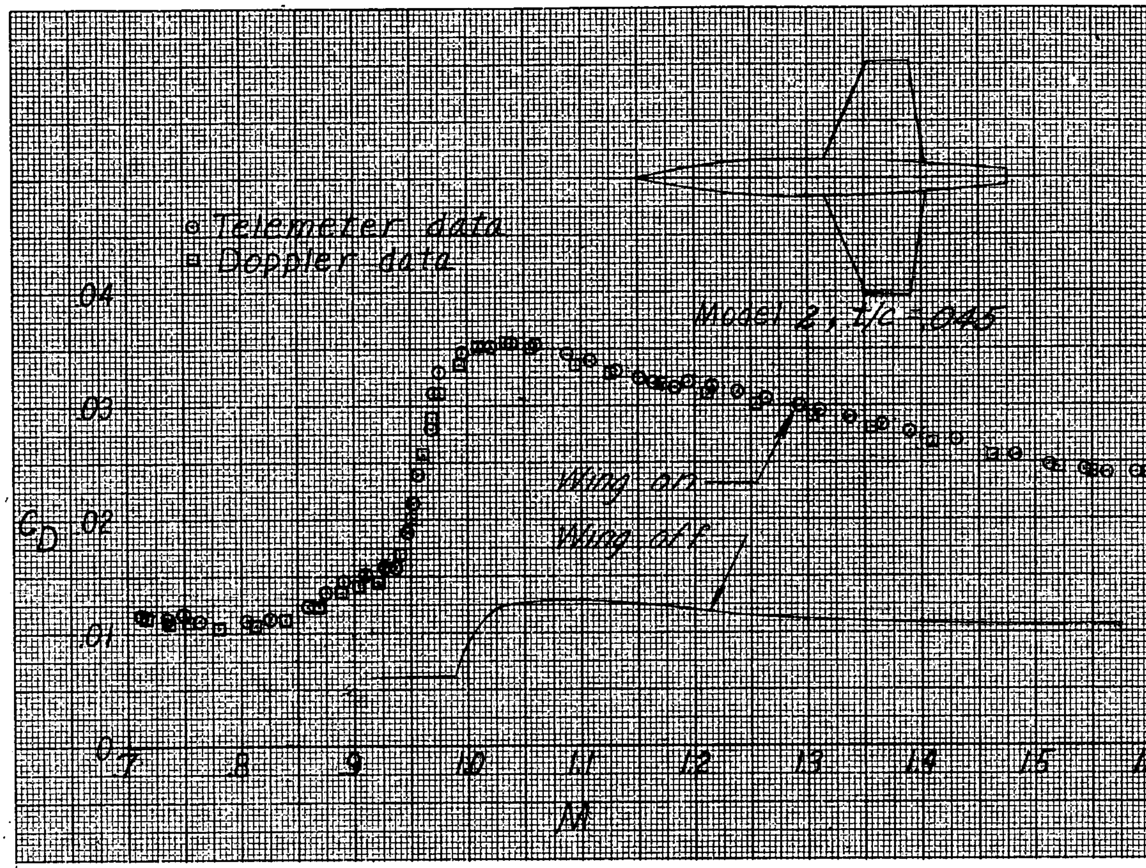

(a) Total drag.

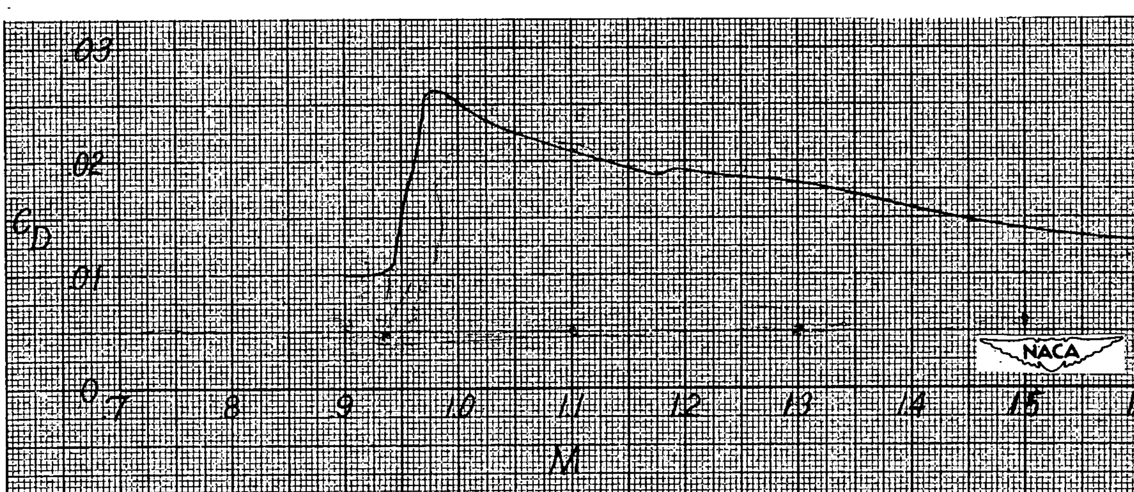

(b) Wing-plus-interference drag.

Figure 5.- Drag of a straight wing on a parabolic body, model 2. C_D based on total wing to fuselage center line.

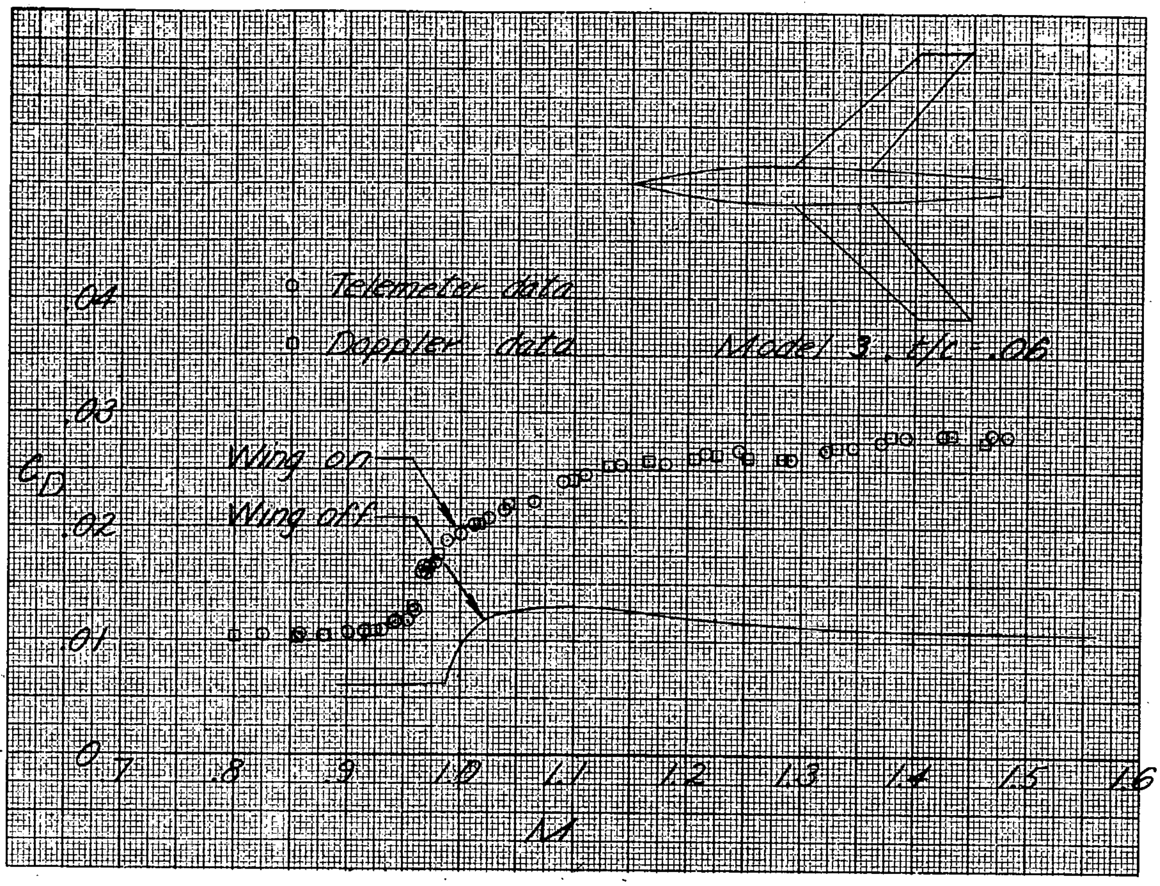

(a) Total drag.

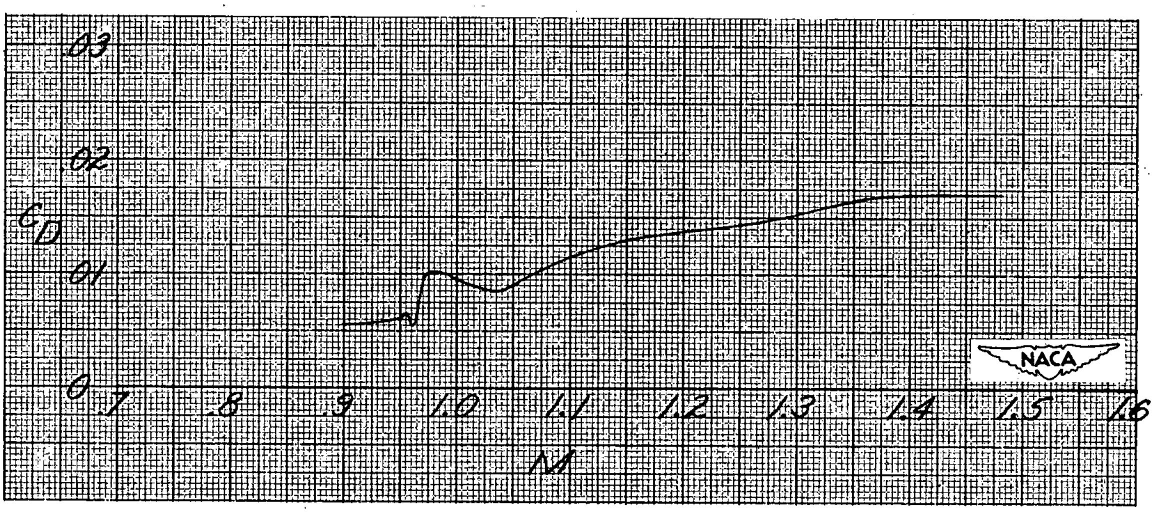

(b) Wing-plus-interference.

Figure 6.- Drag of a 45° swept wing on a parabolic body, model 3. C_D based on total wing to fuselage center line.

[redacted]

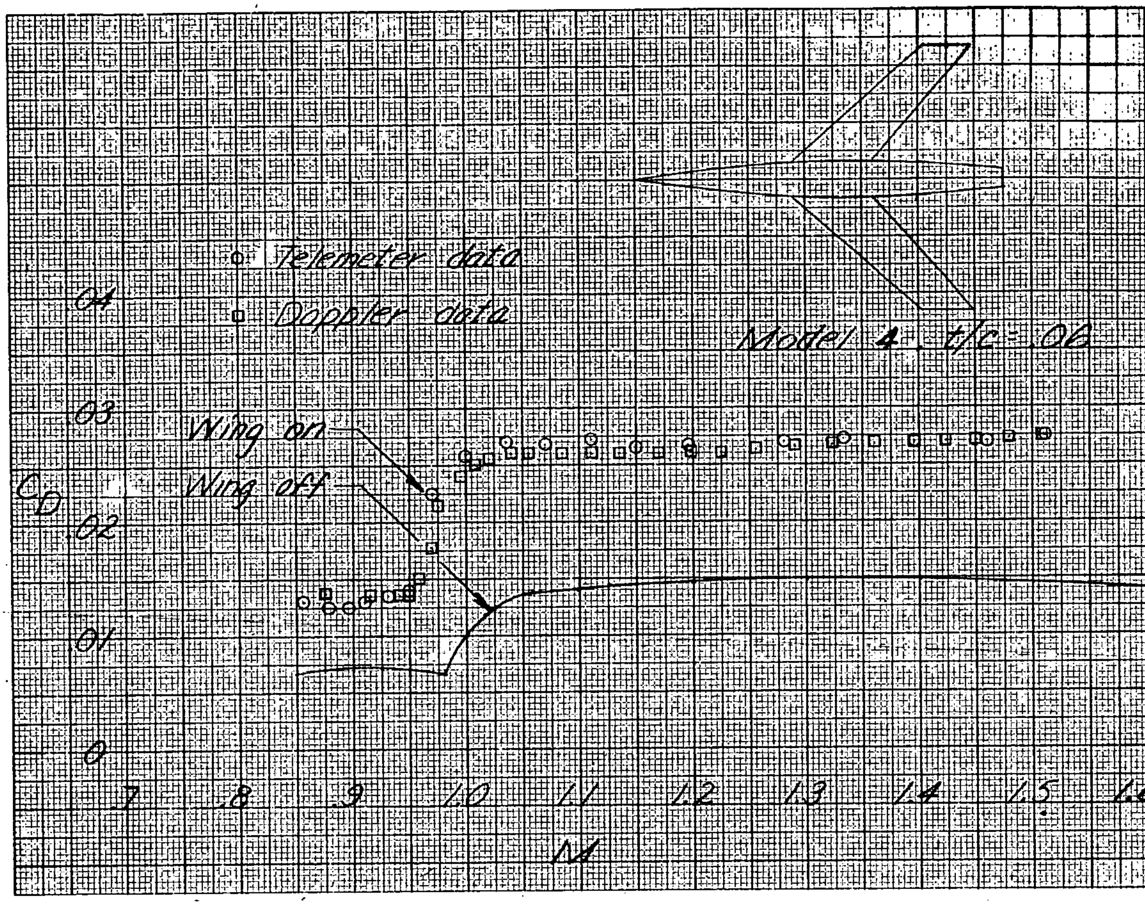

(a) Total drag.

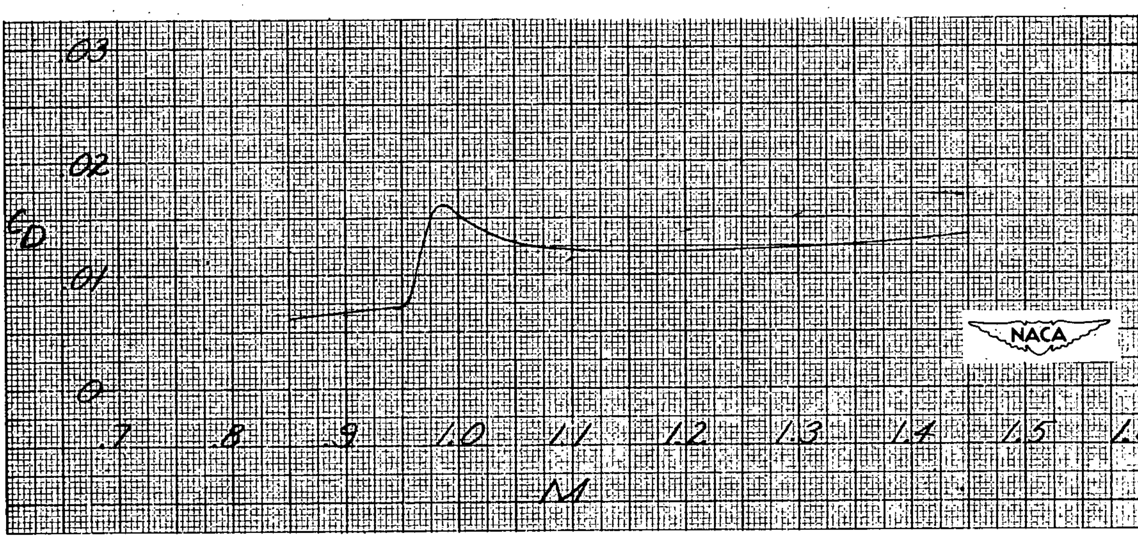

(b) Wing-plus-interference drag.

Figure 7.- Drag of a 45° swept wing on a transonic body, model 4. (See reference 2.) C_D based on total wing to fuselage center line.

[redacted]

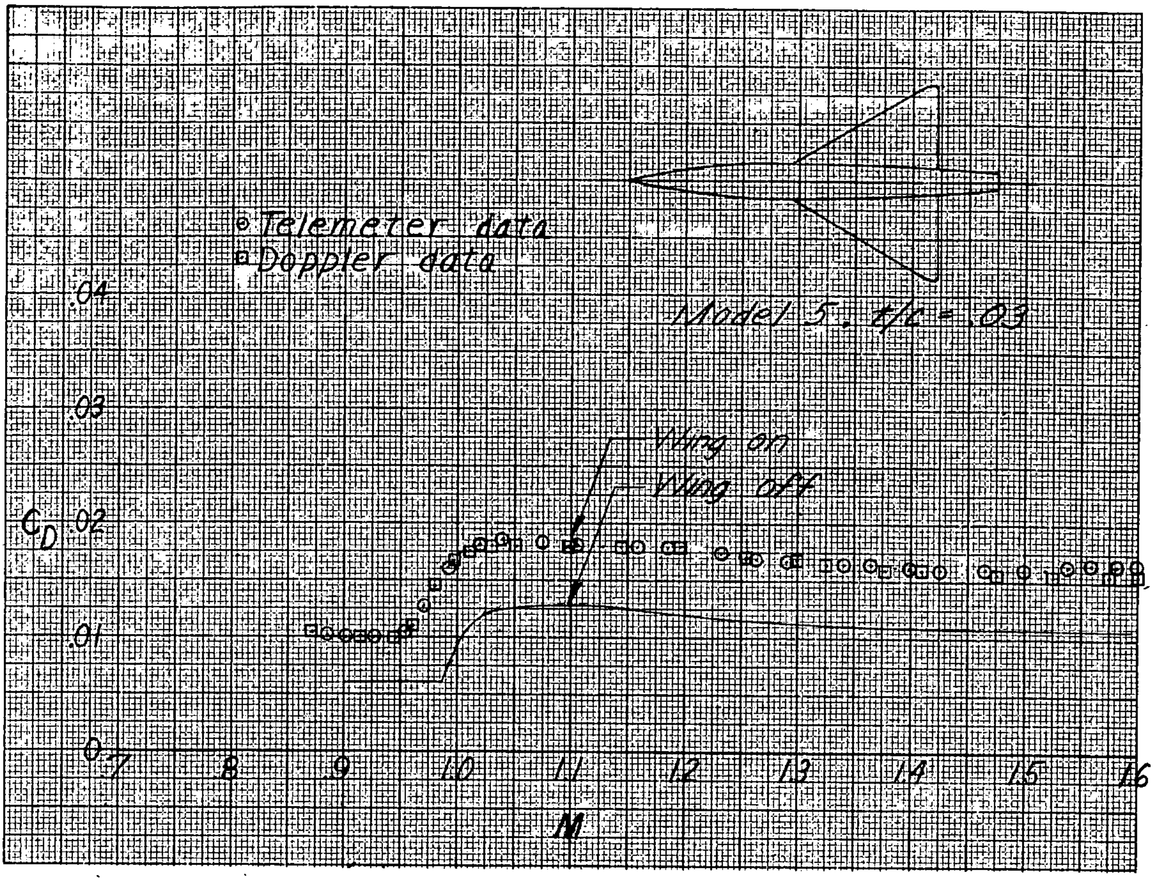

(a) Total drag.

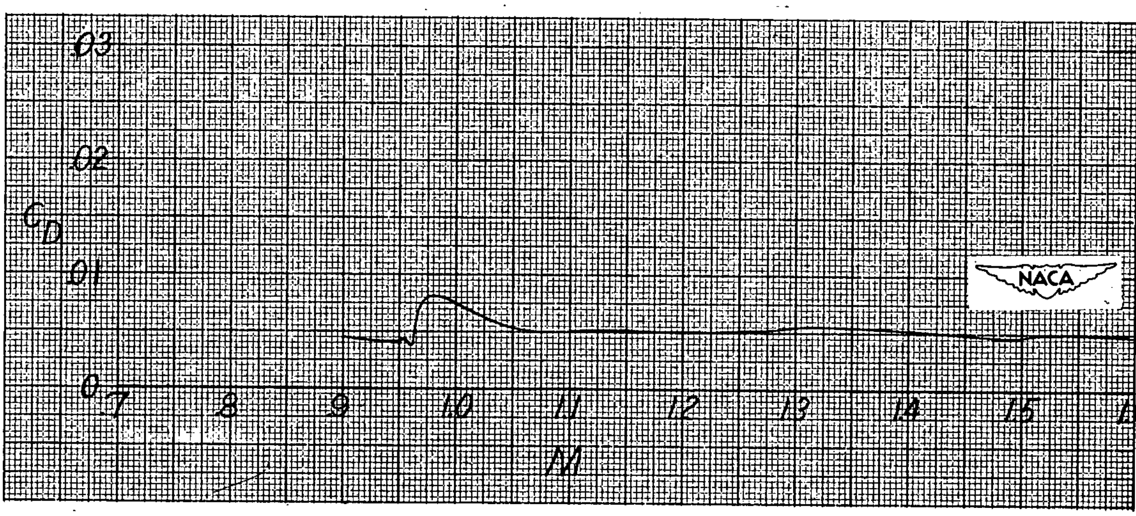

(b) Wing-plus-interference drag.

Figure 8.- Drag of a small 60° delta wing on a parabolic body, model 5. (See reference 1.) C_D based on total wing to fuselage center line.

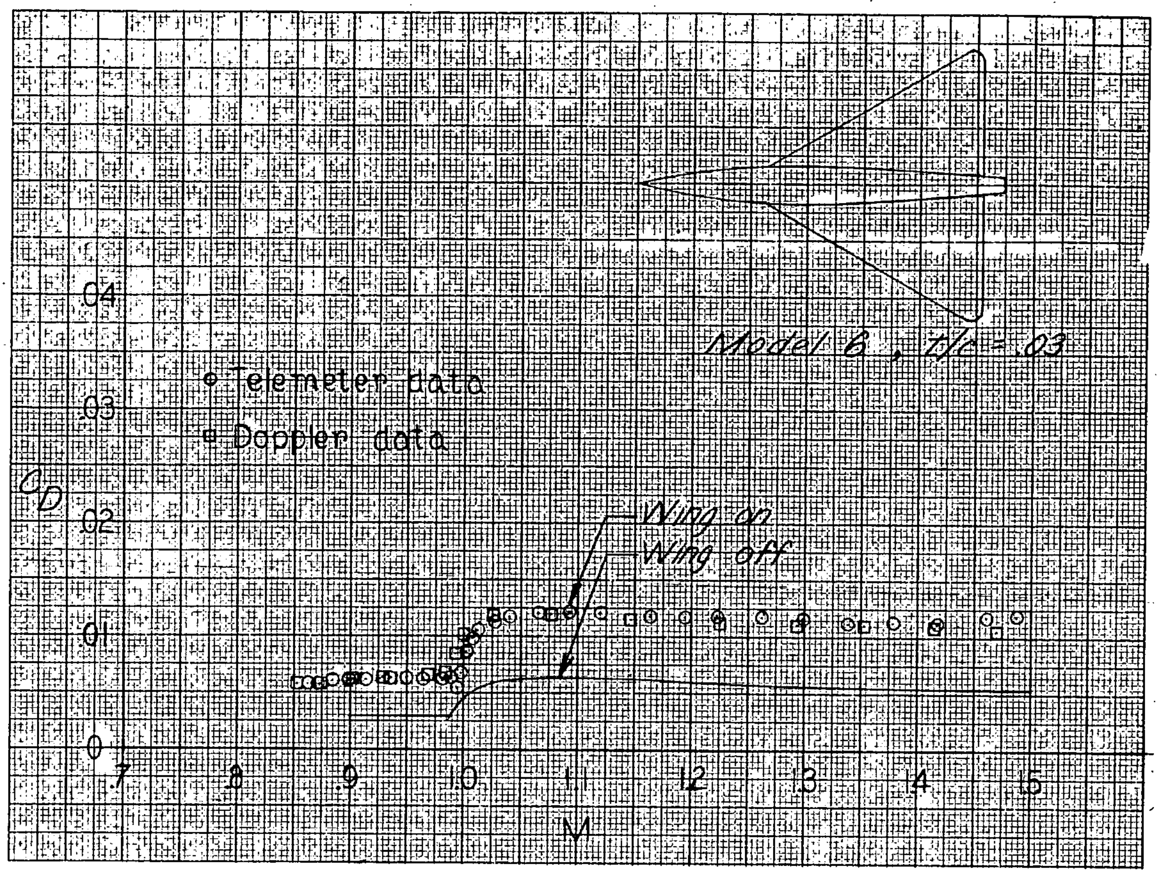

(a) Total drag.

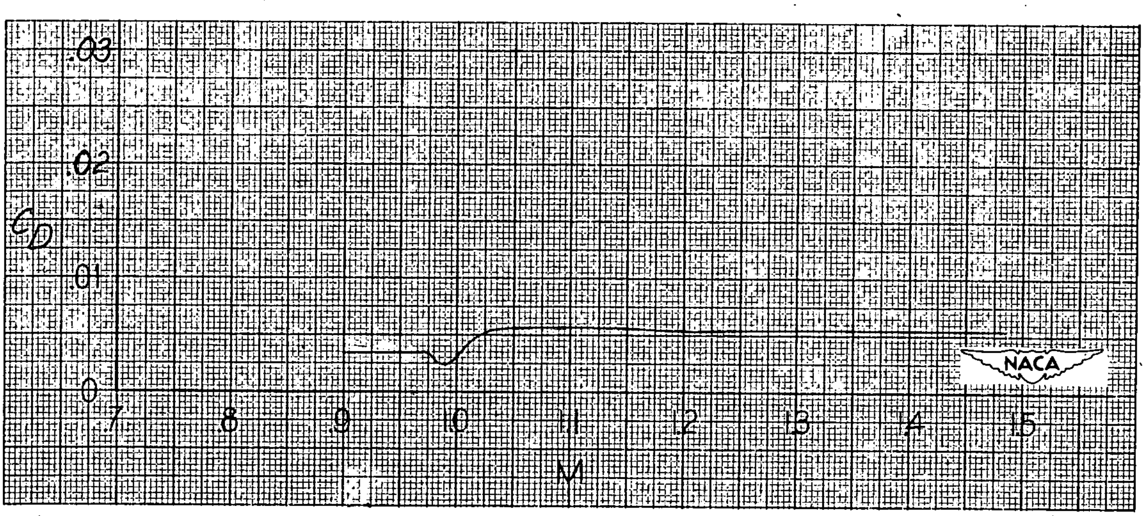

(b) Wing-plus-interference drag.

Figure 9.- Drag of a large 60° delta wing on a parabolic body, model 6. (See reference 1.) C_D based on total wing to fuselage center line.

[redacted]

[redacted]

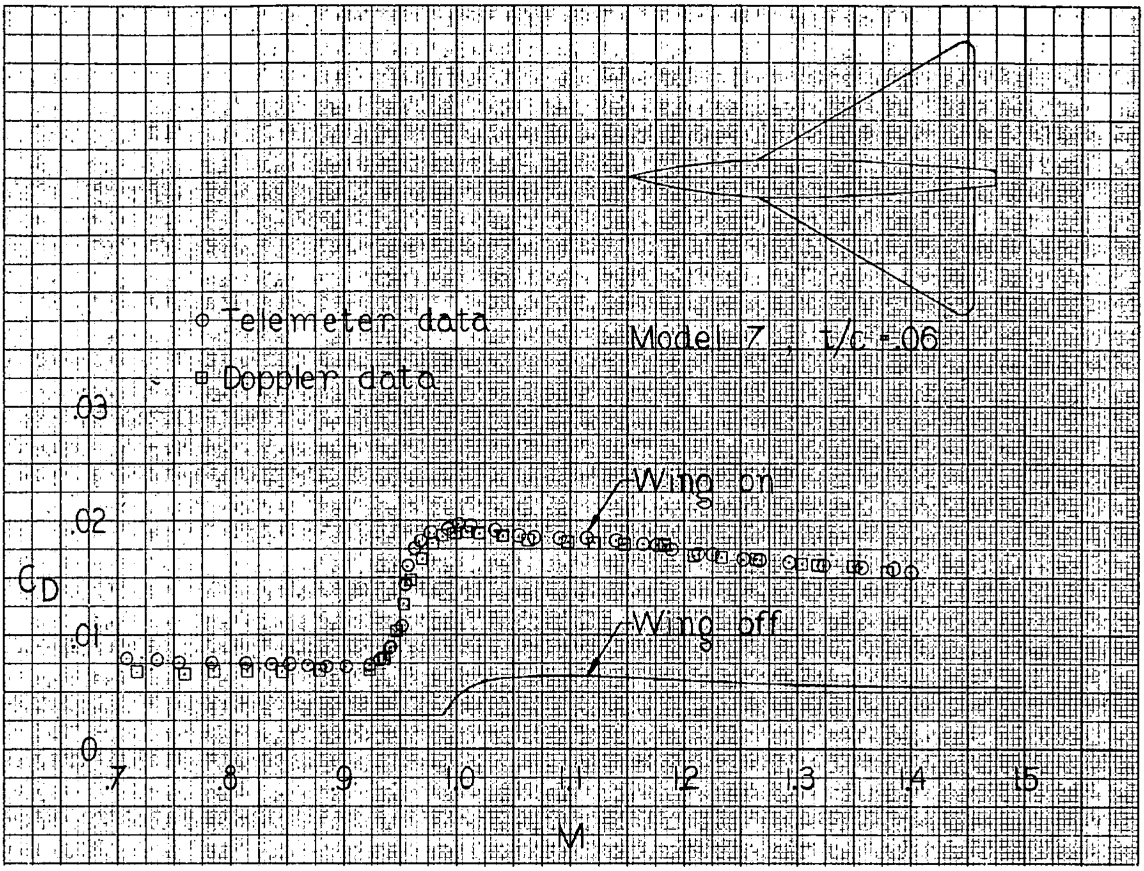

(a) Total drag.

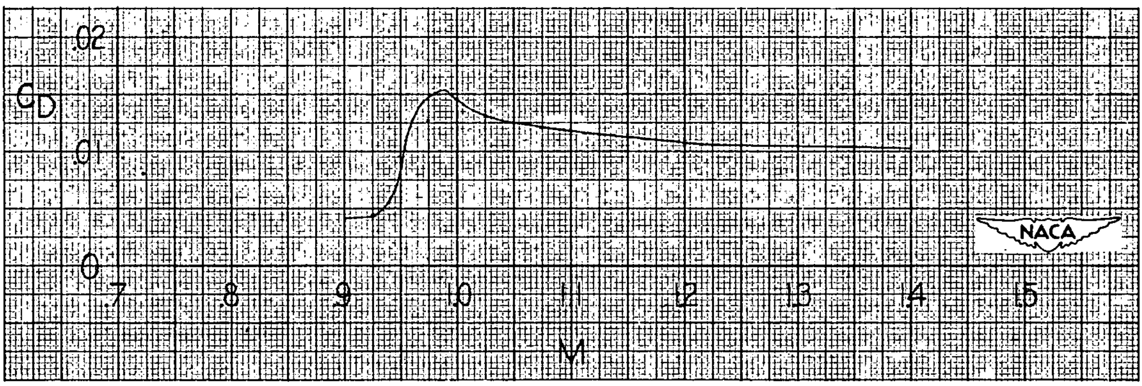

(b) Wing-plus-interference drag.

Figure 10.- Drag of a large 60° delta wing on a parabolic body, model 7. C_D based on total wing to fuselage center line.

[redacted]

[redacted]

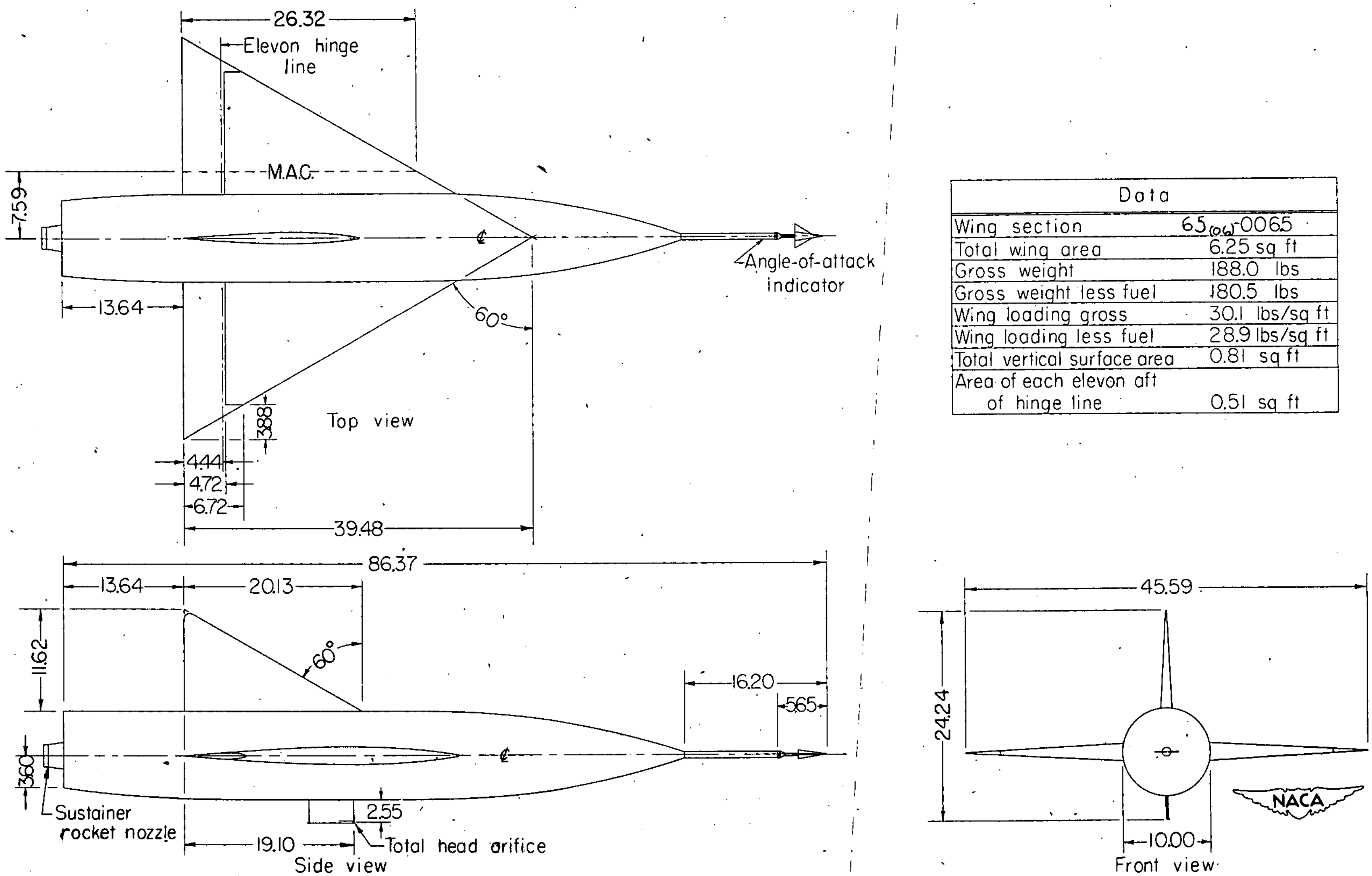

Data	
Wing section	$65_{(06)}$-0065
Total wing area	6.25 sq ft
Gross weight	188.0 lbs
Gross weight less fuel	180.5 lbs
Wing loading gross	30.1 lbs/sq ft
Wing loading less fuel	28.9 lbs/sq ft
Total vertical surface area	0.81 sq ft
Area of each elevon aft of hinge line	0.51 sq ft

Figure 11.- Three-view drawing of model 8. Reference 3. (All dimensions are in inches.)

[redacted]

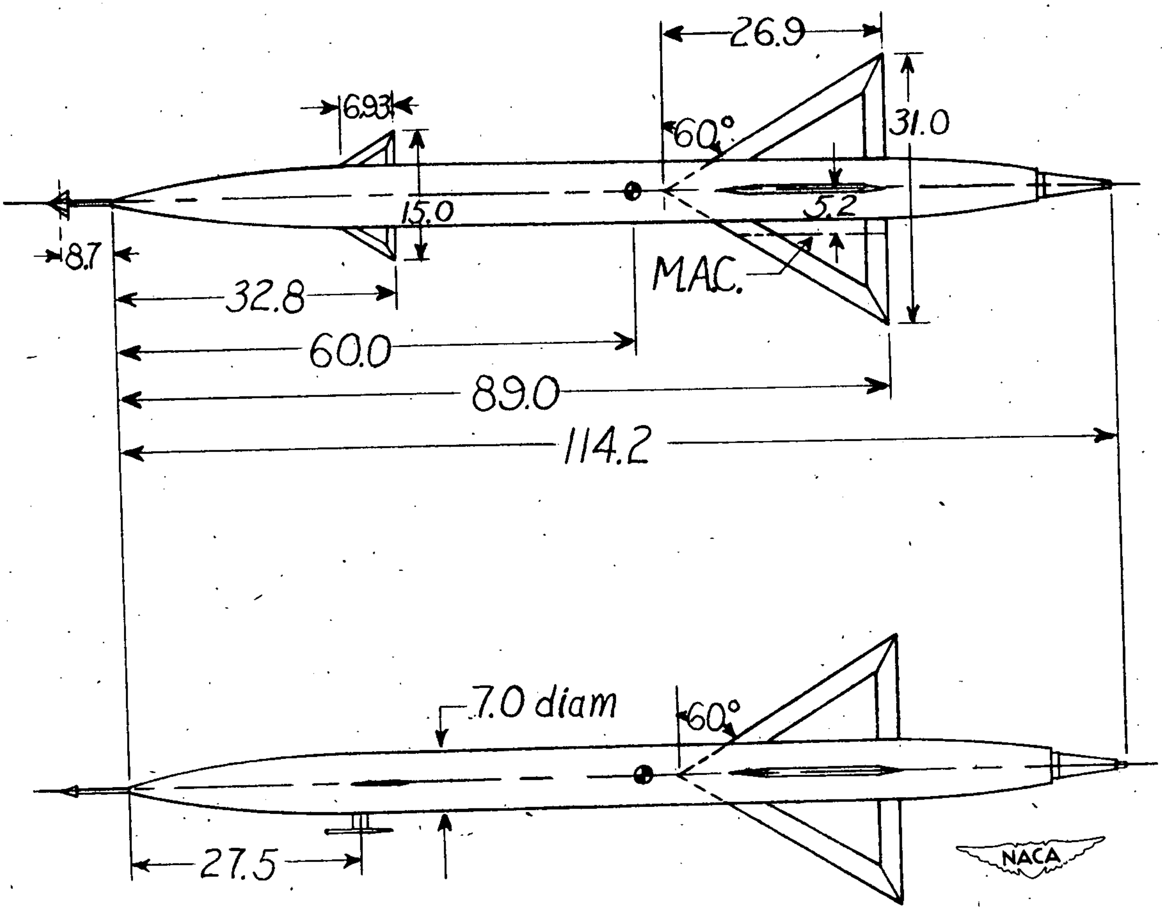

Wing	
S_w, sq ft	2.89
MAC, ft	1.49
$\frac{t}{c}$ (average)	0.06
Canard control surfaces	
S_e, sq ft	0.192
MAC, ft	0.387
$\frac{t}{c}$ (average)	0.06

Figure 12.- General arrangement of model 9. All dimensions in inches. Reference 4.

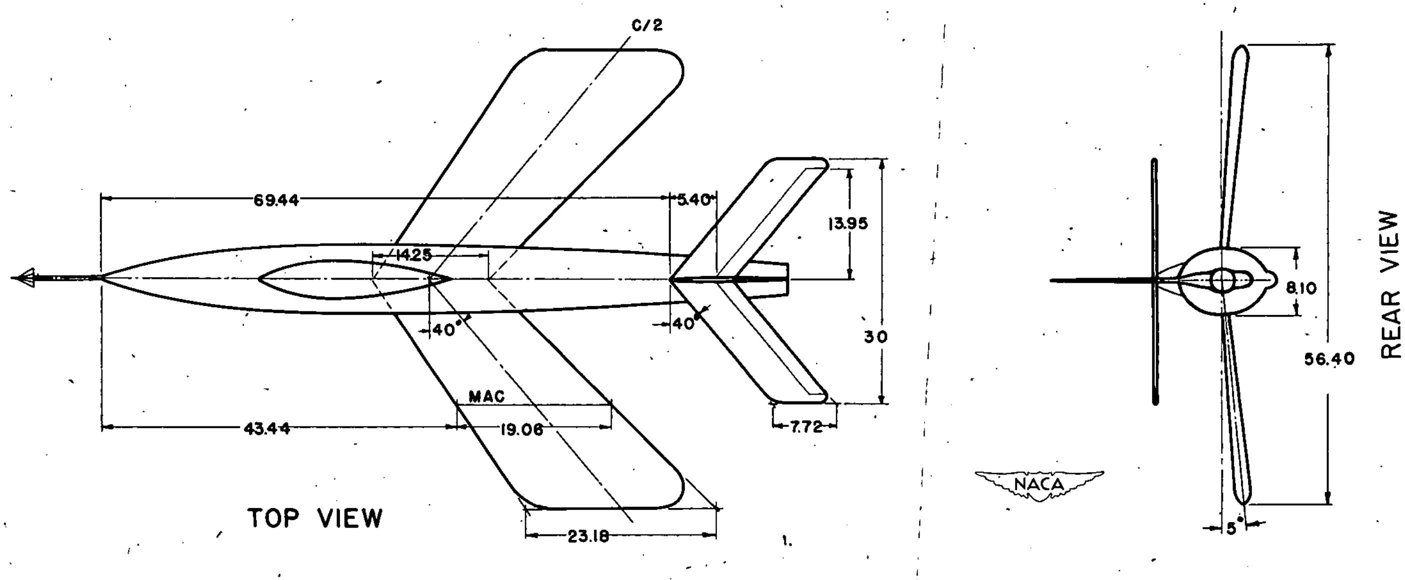

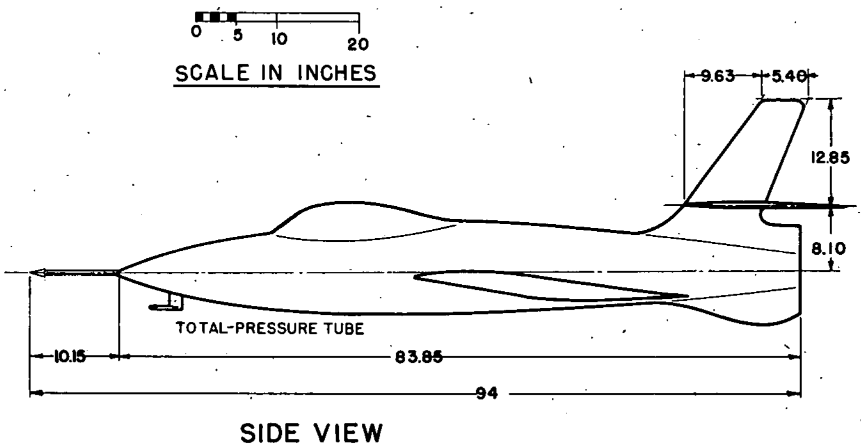

Wing:
- Area, sq ft 7.20
- Aspect ratio 3.07
- Taper ratio 1.626
- Airfoil, low drag section, t/c (streamwise) . . . 0.076

Horizontal tail:
- Area, sq ft 1.57
- Aspect ratio 3.98
- Taper ratio 1.00
- Airfoil, low drag section, t/c (streamwise) . . . 0.076

Vertical tail:
- Area, sq ft 1.085

Figure 13.- General arrangement of model 10. (See reference 5.)

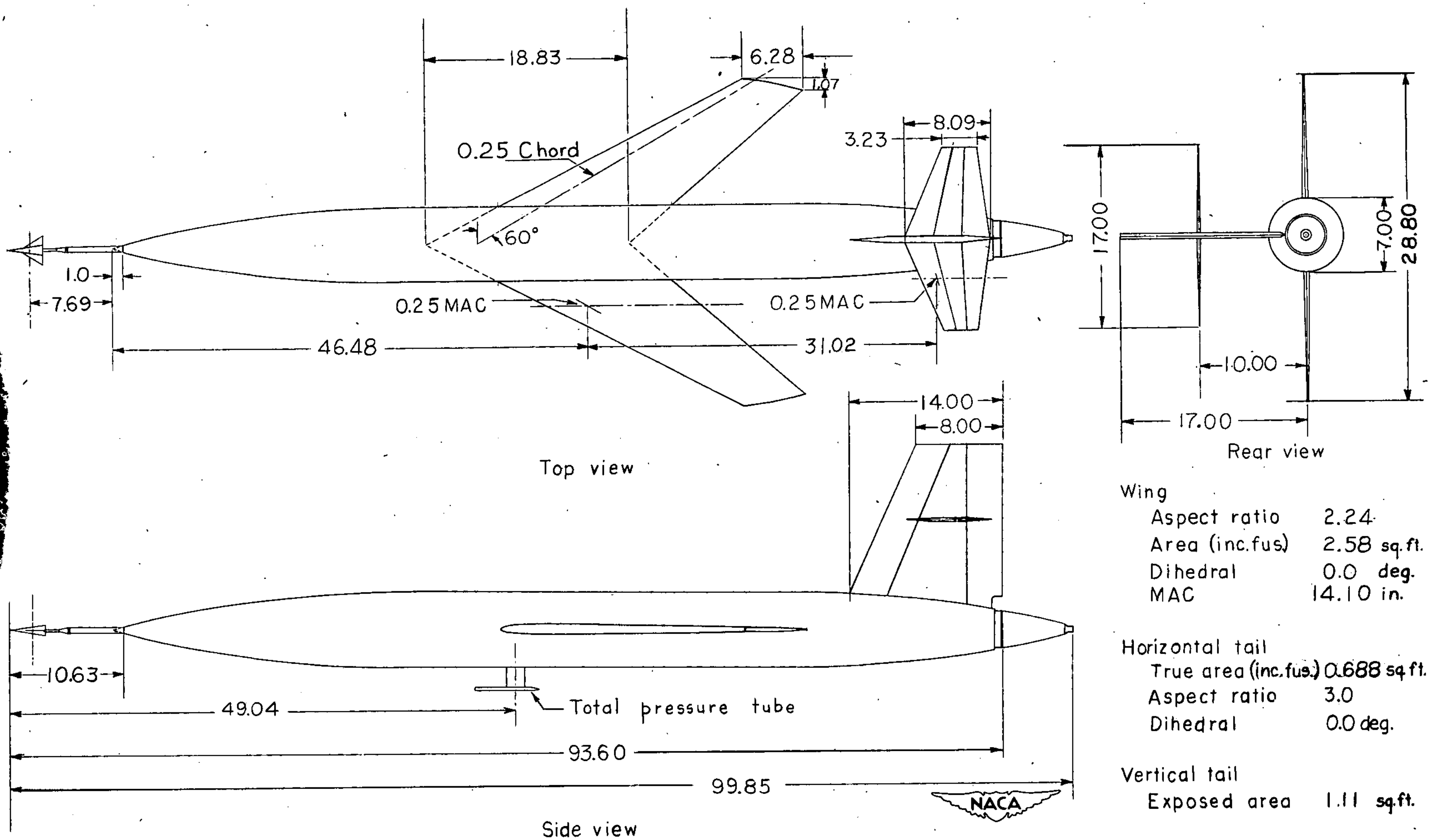

Figure 14.- General arrangement of model 11. Wing of 64-series airfoil; $\frac{t}{c} = 0.063$ streamwise at wing-body juncture; $\frac{t}{c} = 0.049$ streamwise at tip. (All dimensions are in inches.)

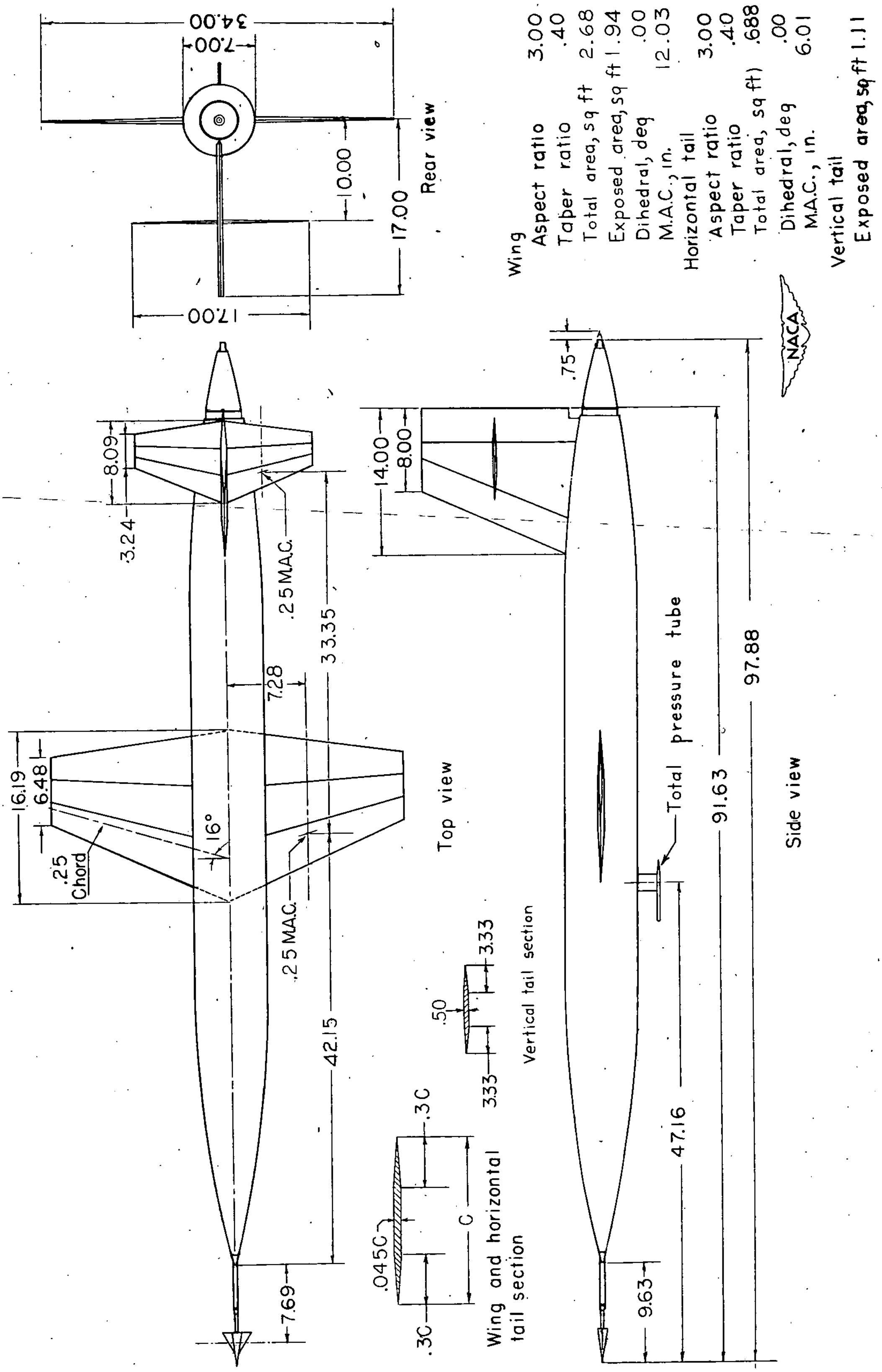

Figure 15.- General arrangement of model 12. (See references 6 and 7.) (All dimensions are in inches.)

[redacted]

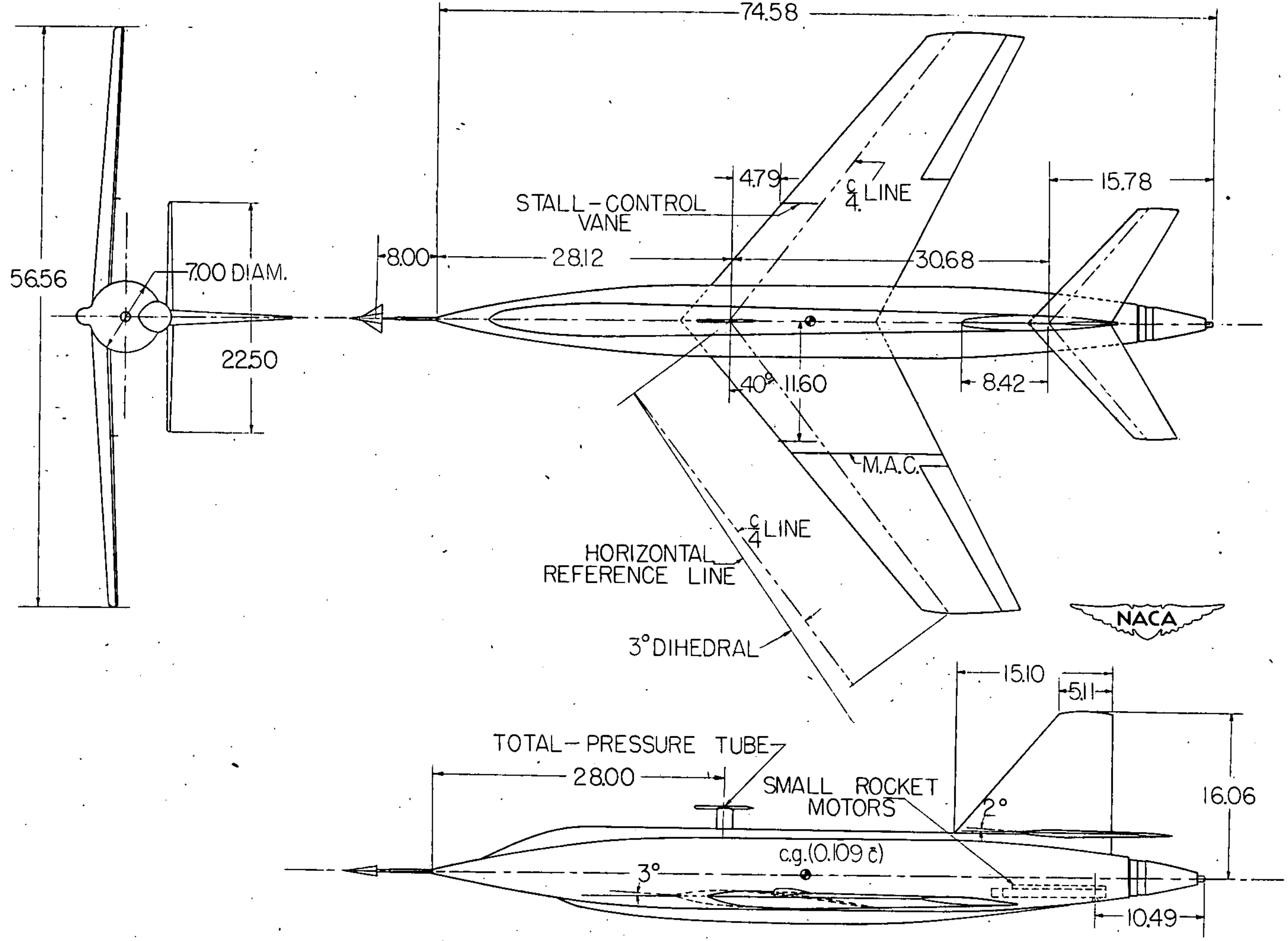

(a) General arrangement.

Figure 16.- Model 18 (reference 8).

[redacted]

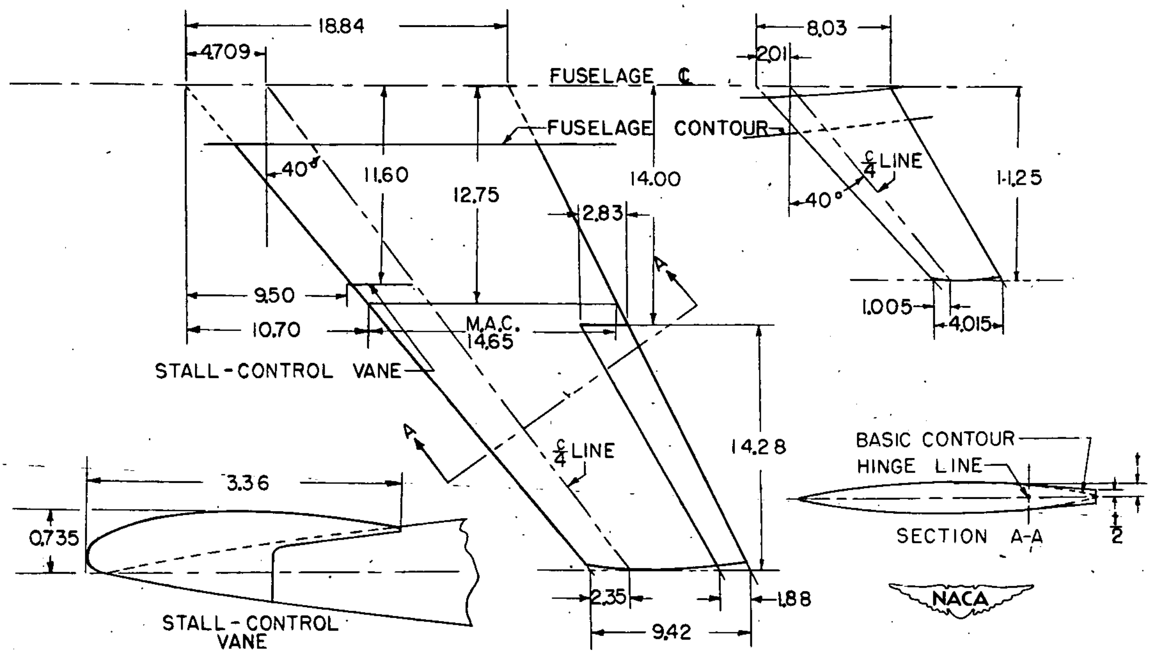

Wing:
Area, sq ft 5.56
Aspect ratio 4.00
Taper ratio 0.50
Airfoil section, normal
to c/4 line, circular-arc,
10 percent thick

Horizontal tail:
Area, sq ft 0.938
Aspect ratio 3.72
Taper ratio 0.50
Airfoil section, normal
to c/4 line . . . NACA 65-008

Vertical tail:
Area, sq ft 0.966

(b) Wing and tail details.

Figure 16.- Concluded. Model 18.

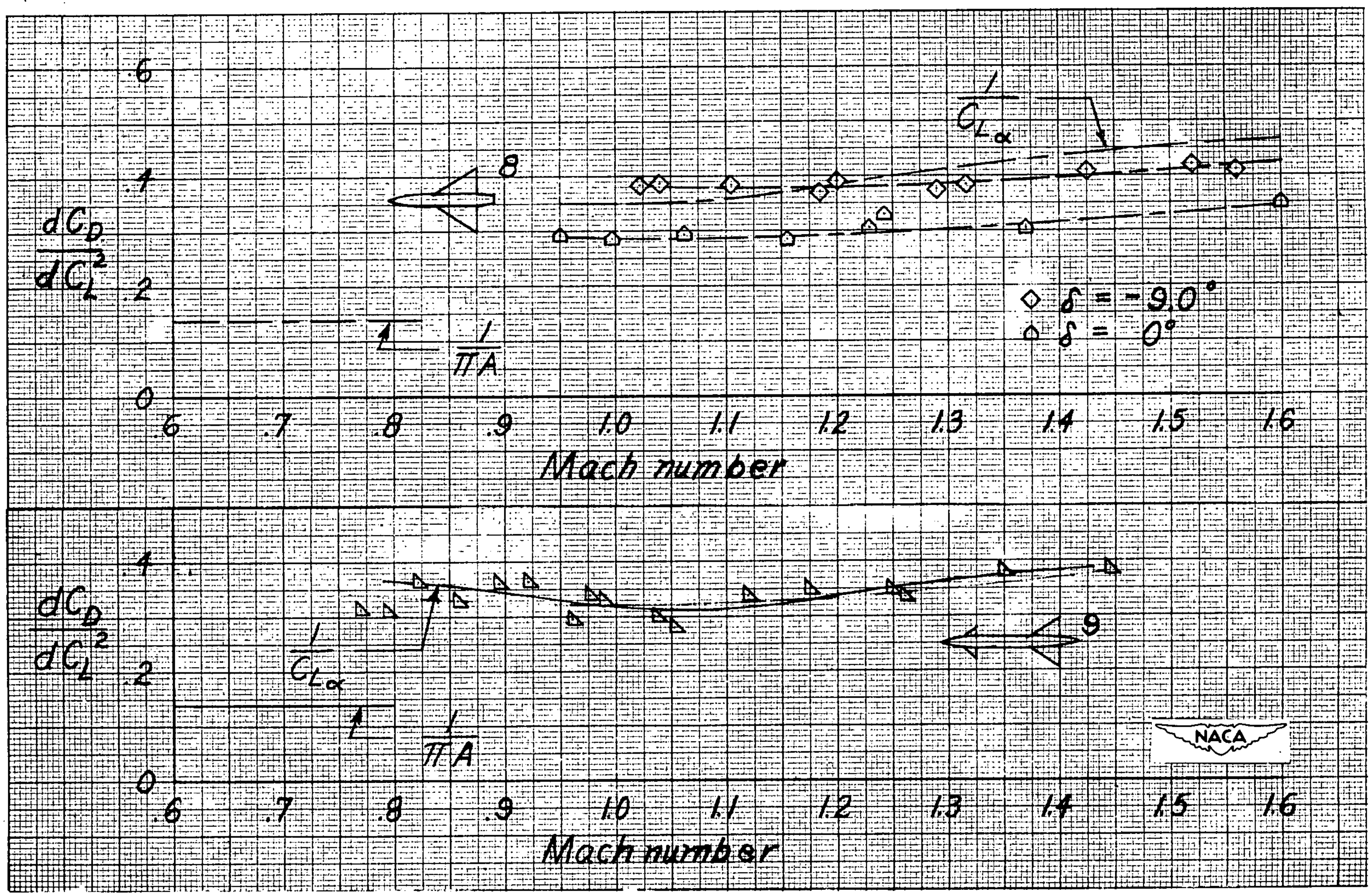

Figure 17.- Drag due to lift of several delta-wing configurations. C_D based on total wing area to body center line.

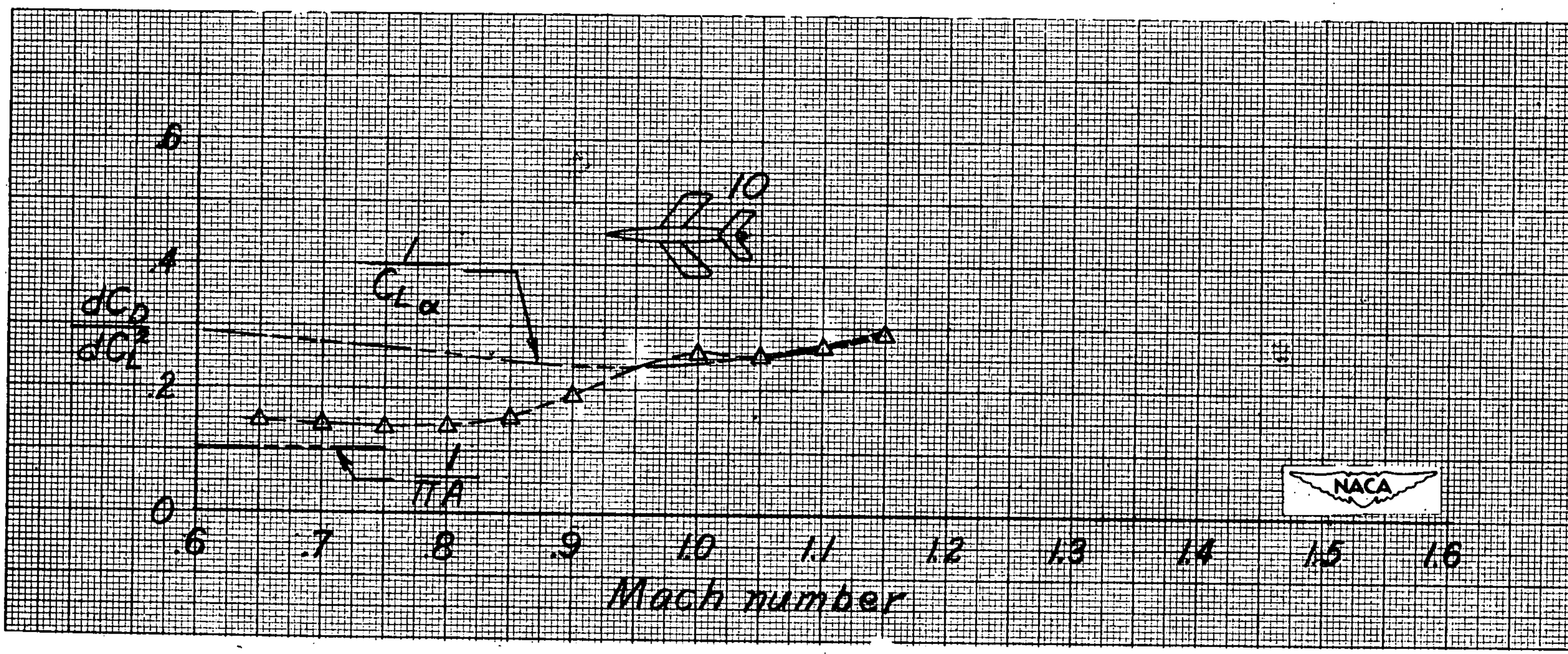

Figure 18.- Drag due to lift of a sweptback-wing configuration. C_D based on total wing area to body center line.

[redacted]

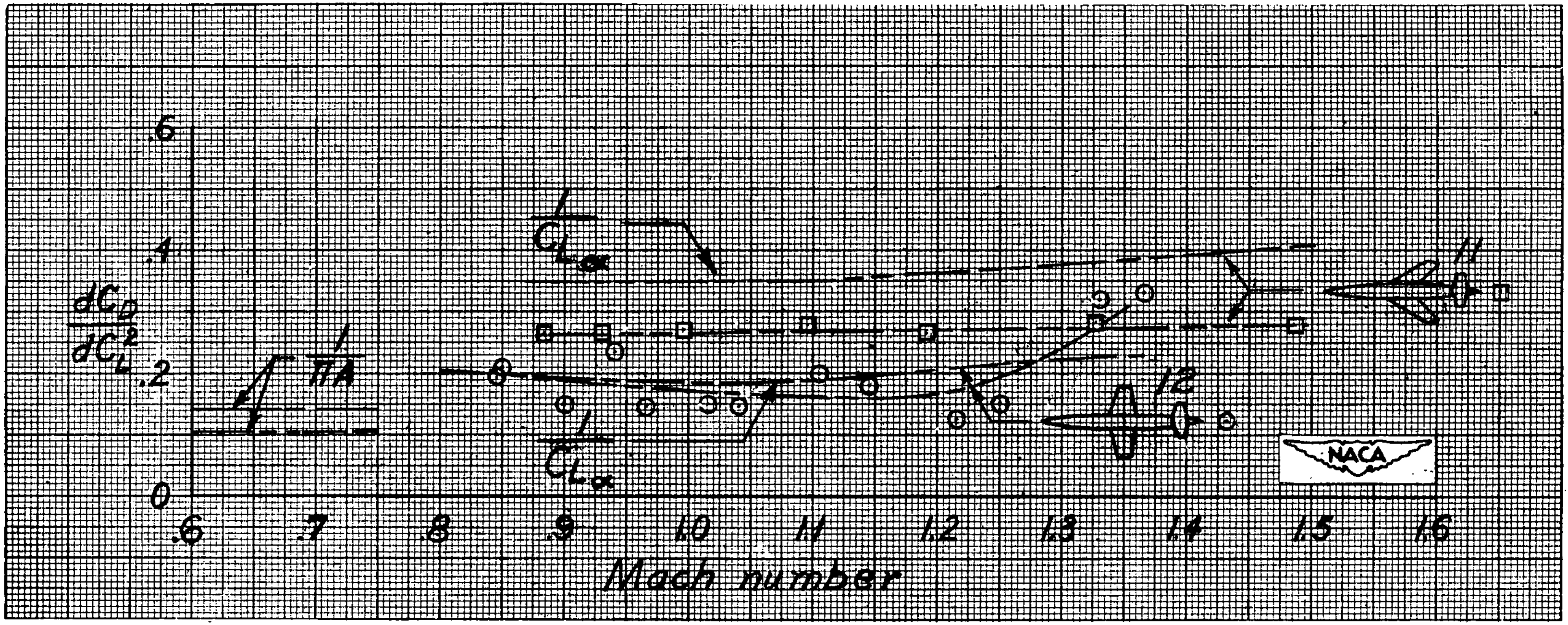

Figure 19.- Drag due to lift of a straight and a sweptback wing with the same fuselage configuration. C_D based on total wing area to body center line.

[redacted]

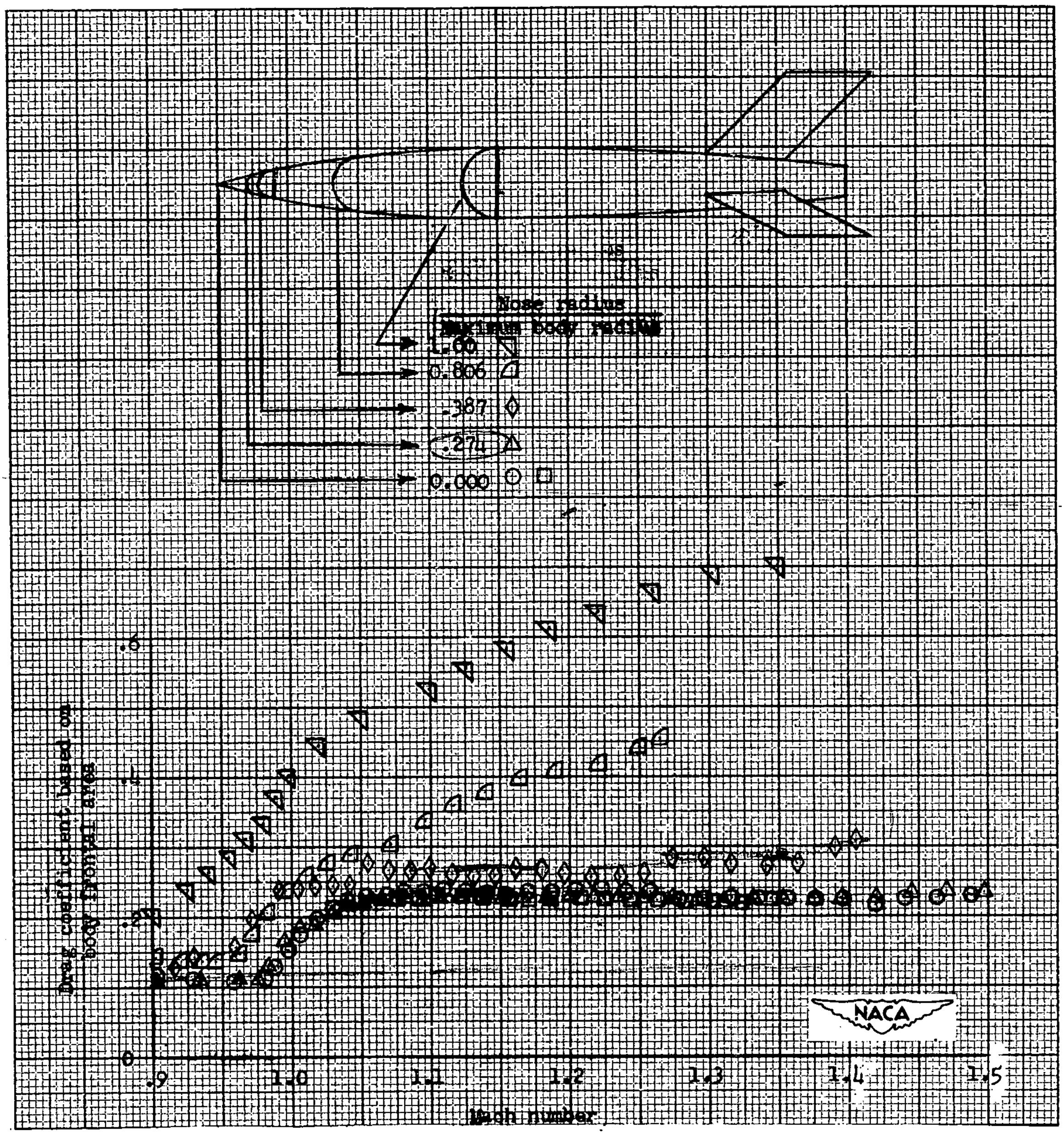

Figure 20.- Drag changes due to rounding off the nose of a fin-stabilized parabolic body of revolution of fineness ratio 8.91. Dimensions of the pointed-nose body may be found in reference 9. Model 13.

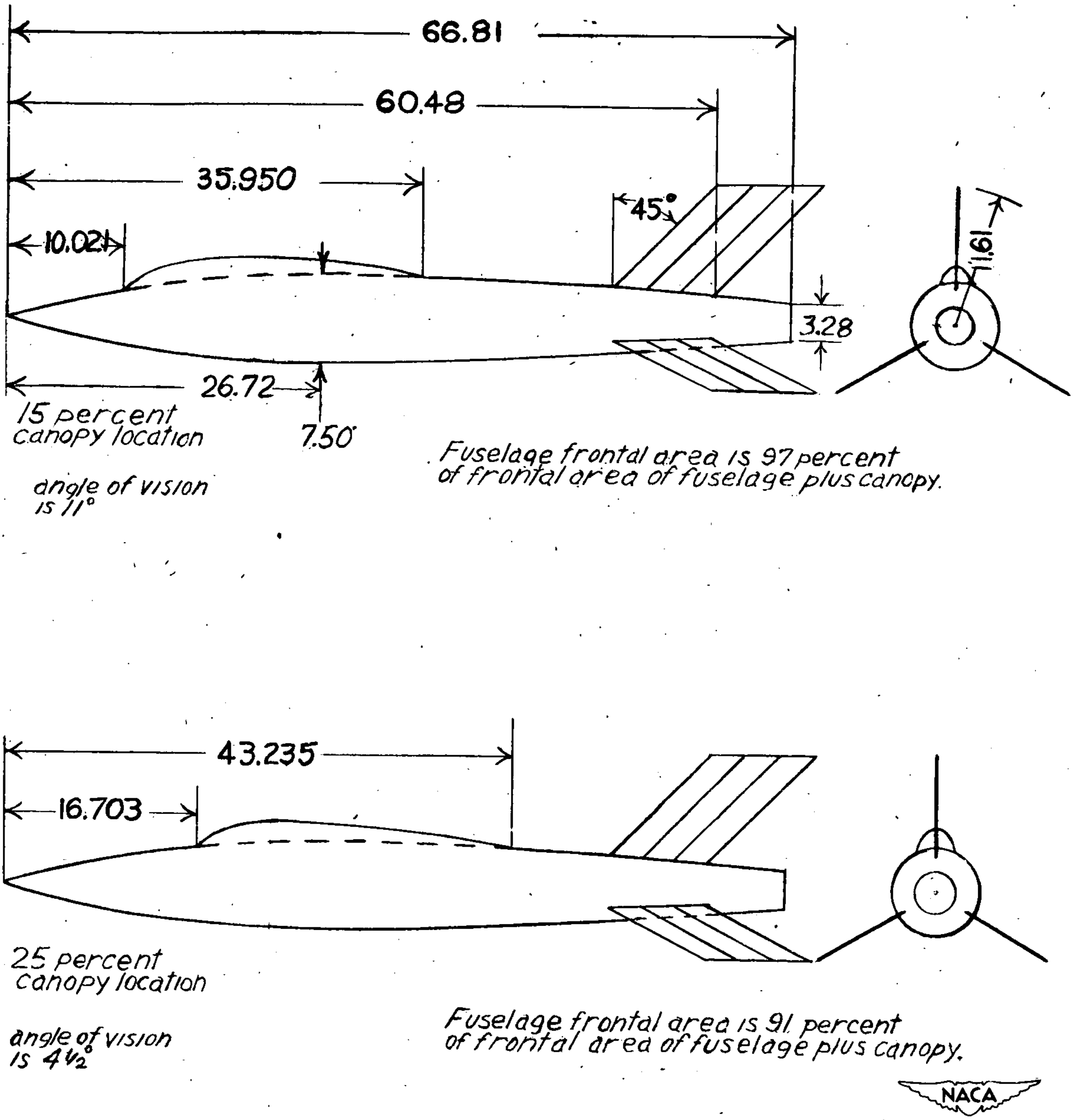

(a) General arrangement.

Figure 21.- Canopies are fineness-ratio-7.82 parabolic bodies (with maximum diameter at 15.5 percent body length) bent to conform to the contour of the fuselage. The fuselage is identical to the parabolic body reported in reference 9. Model 14.

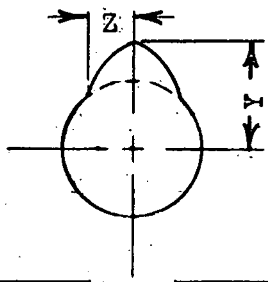

Coordinates
15 percent canopy

Fuselage Station	Z	Y
10.021	0	2.285
10.500	0.450	2.818
11.000	0.830	3.282
12.000	1.365	3.977
14.000	1.705	4.605
16.000	1.781	4.927
18.000	1.640	5.050
20.000	1.560	5.073
22.000	1.455	5.088
24.000	1.344	5.055
26.000	1.182	4.930
28.000	1.000	4.748
30.000	0.805	4.541
32.000	0.560	4.274
34.000	0.285	3.965
35.950	0	3.645

Coordinates
25 percent canopy

Fuselage Station	Z	Y
16.703	0	3.223
17.000	0.260	3.513
18.000	0.915	4.375
20.000	1.602	5.115
22.000	1.690	5.323
24.000	1.685	5.396
26.000	1.620	5.368
28.000	1.531	5.279
30.000	1.415	5.151
32.000	1.291	5.005
34.000	1.120	4.800
36.000	0.925	4.562
38.000	0.715	4.298
40.000	0.460	3.979
42.000	0.180	3.624
43.235	0	3.392

NACA

(b) Coordinates of canopy used. Model 14.

Figure 21.- Concluded.

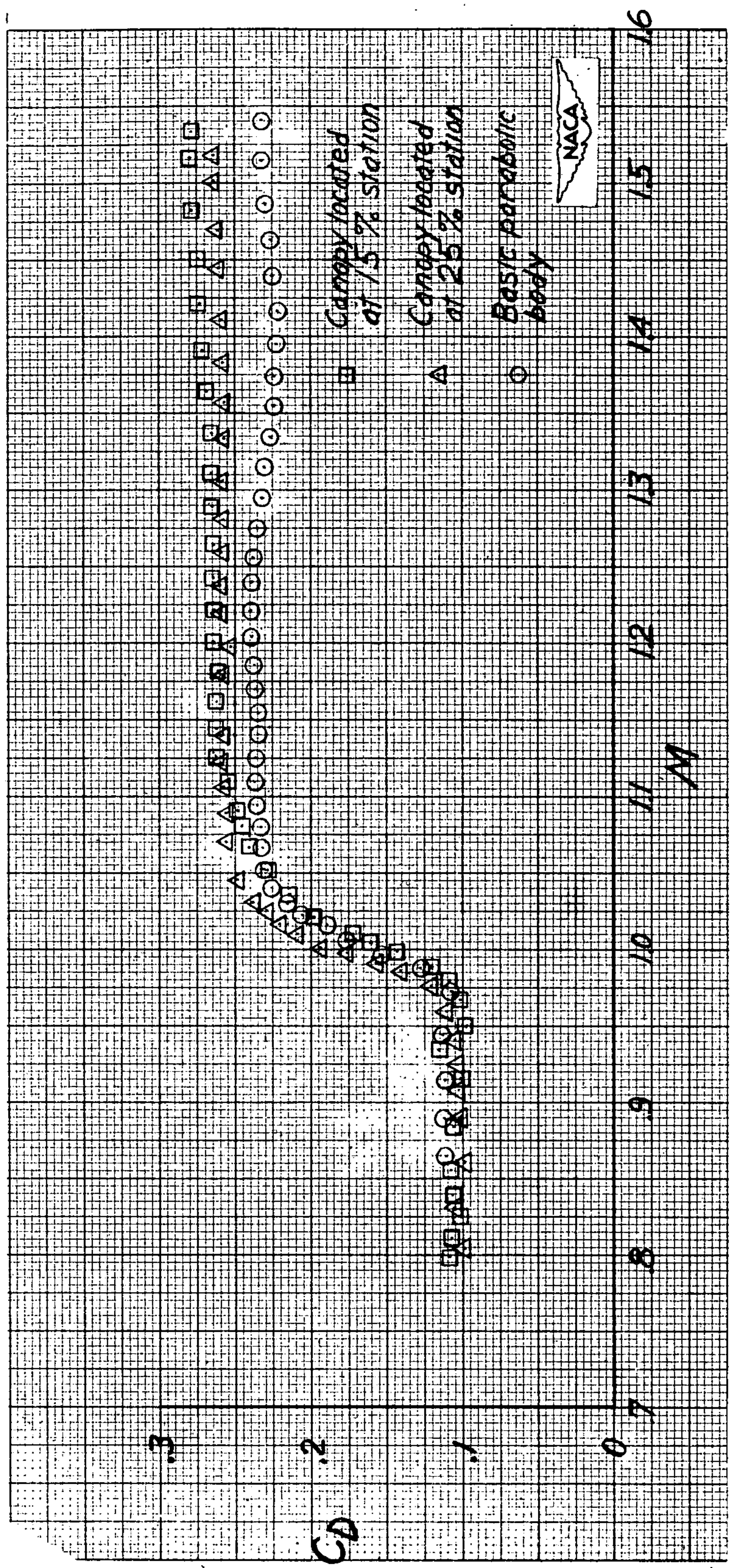

Figure 22.- Total configuration drag coefficient of body-canopy configurations, model 14. C_D based on frontal area of basic body.

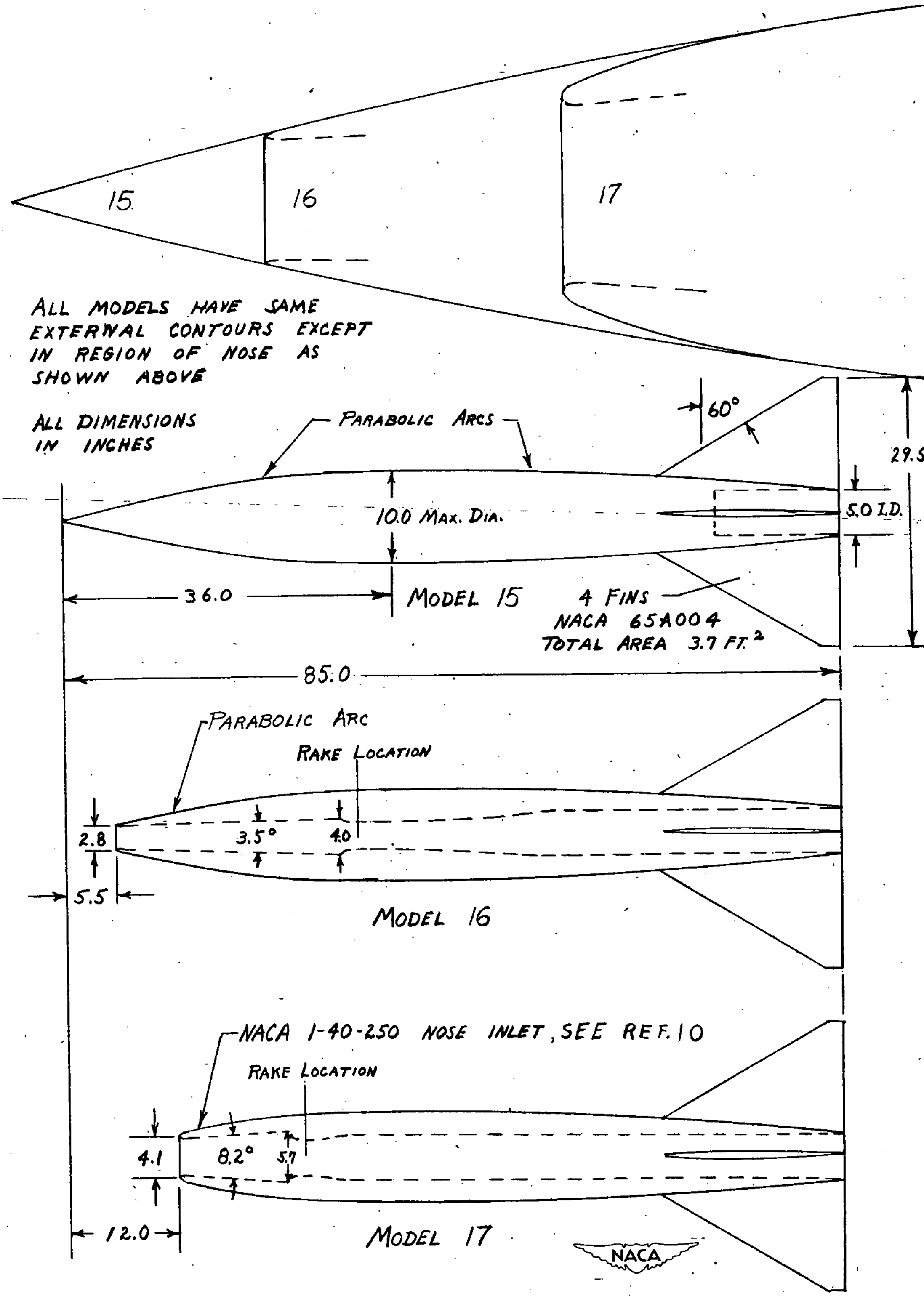

Figure 23. General arrangement of models 15, 16, and 17.

[redacted]

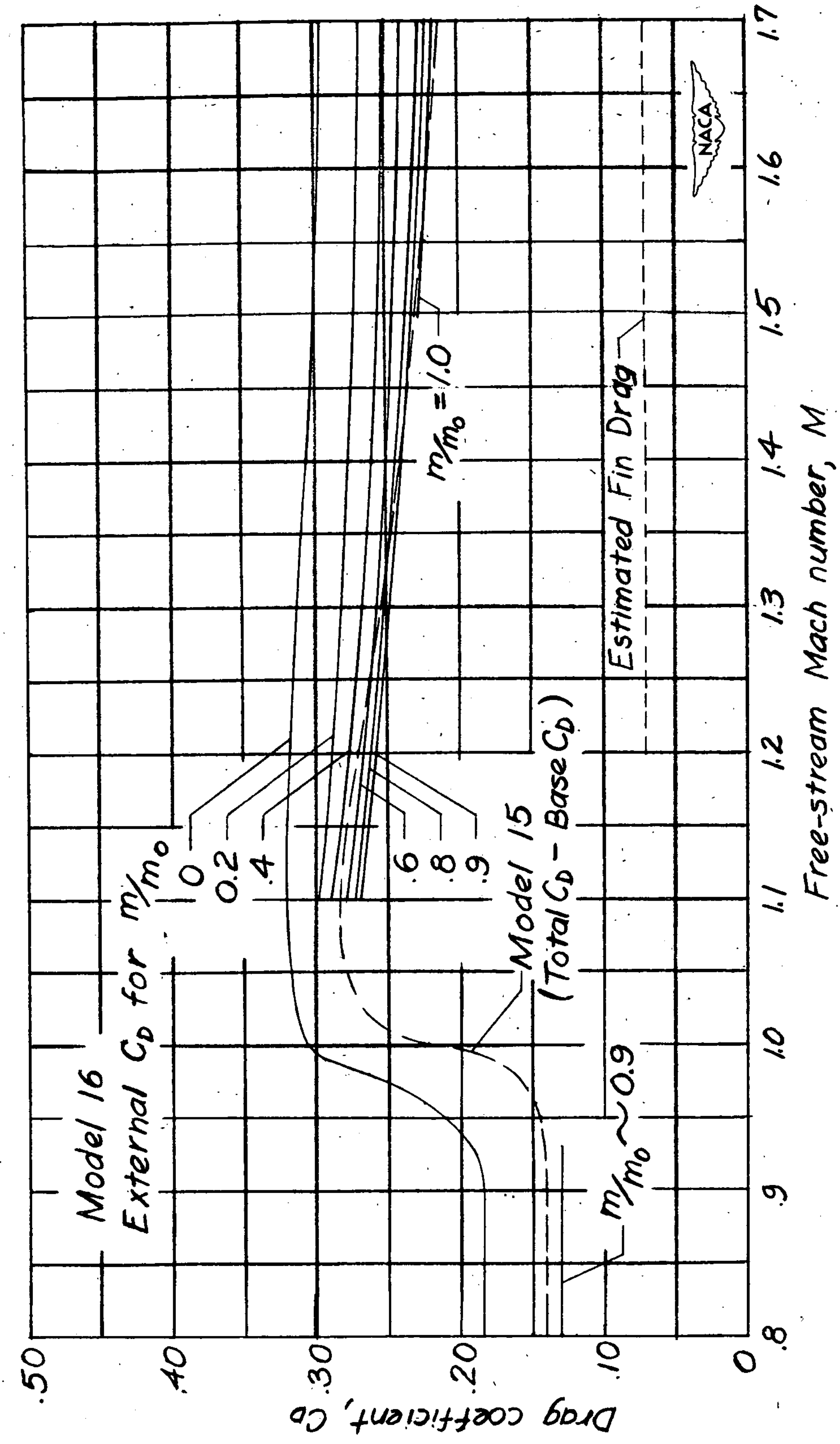

Figure 24.- Variation of external drag coefficient with Mach number for several mass-flow ratios for model 16. C_D based on body frontal area. (Data for medium flow rates at $M < 1.1$ still being reduced.)

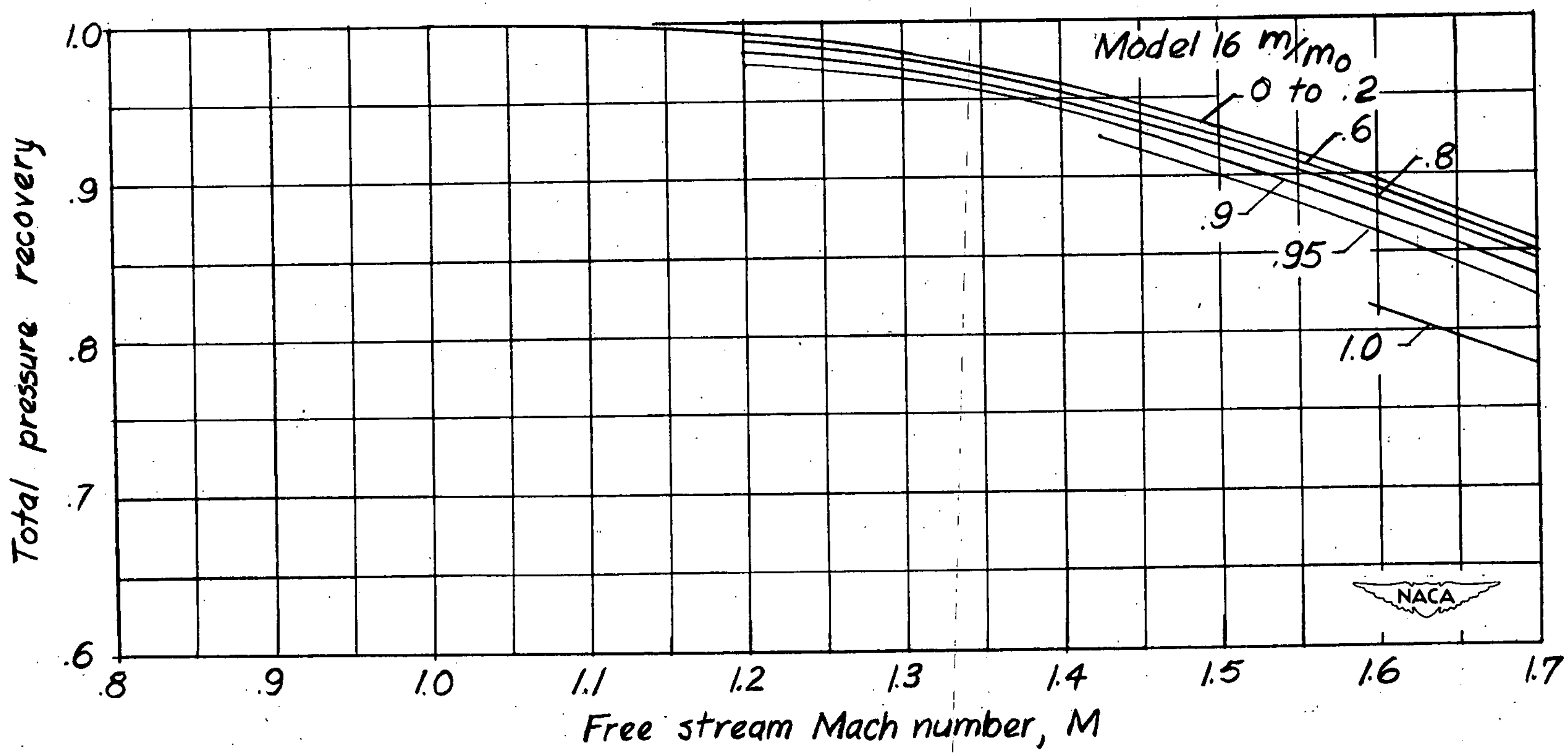

Figure 25.- Variation of total-pressure recovery with Mach number for several mass-flow ratios for model 16. (Data for lower Mach numbers still being reduced.)

[redacted]

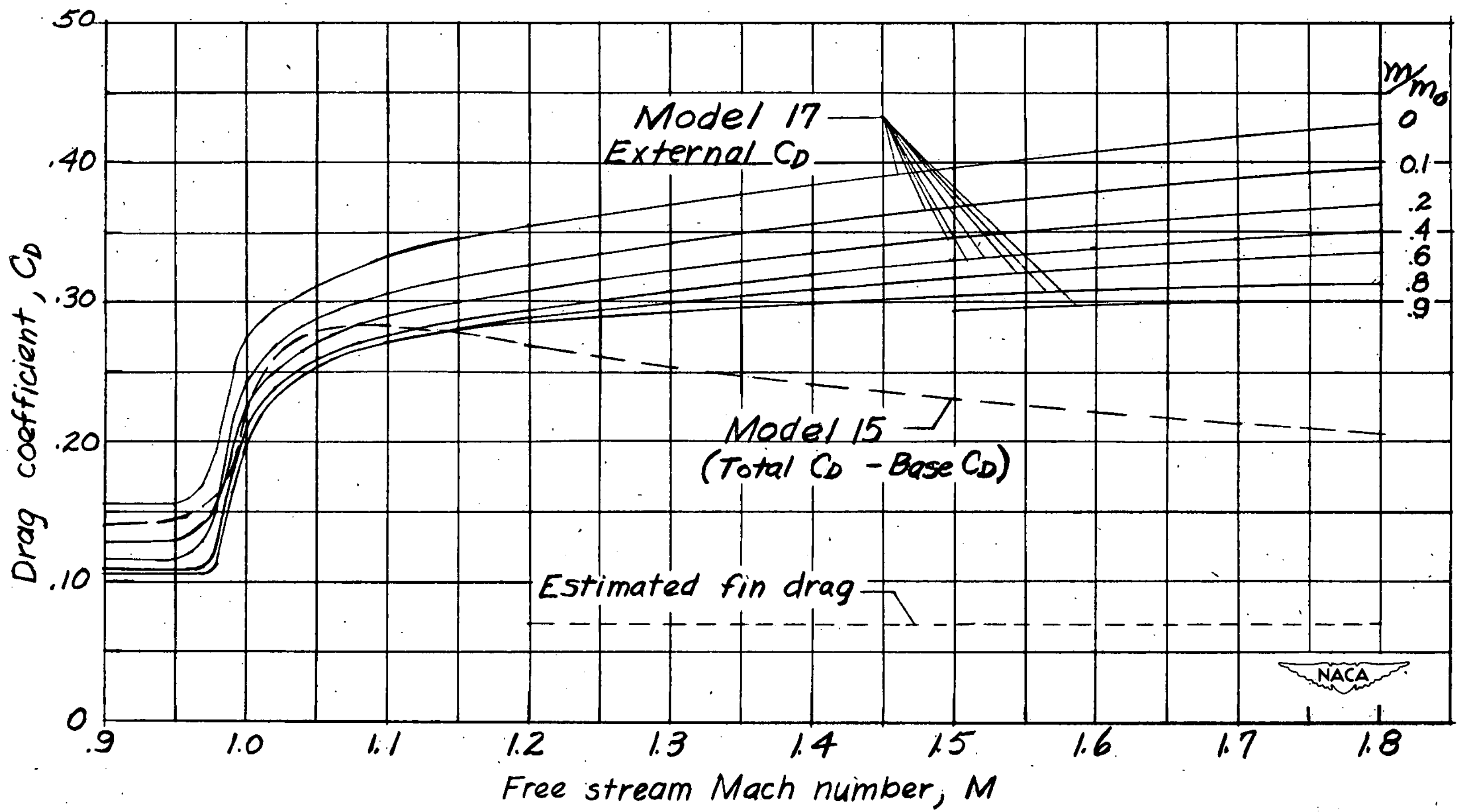

Figure 26.- Variation of external drag coefficient with Mach number for several mass-flow ratios for model 17. C_D based on body frontal area.

[redacted]

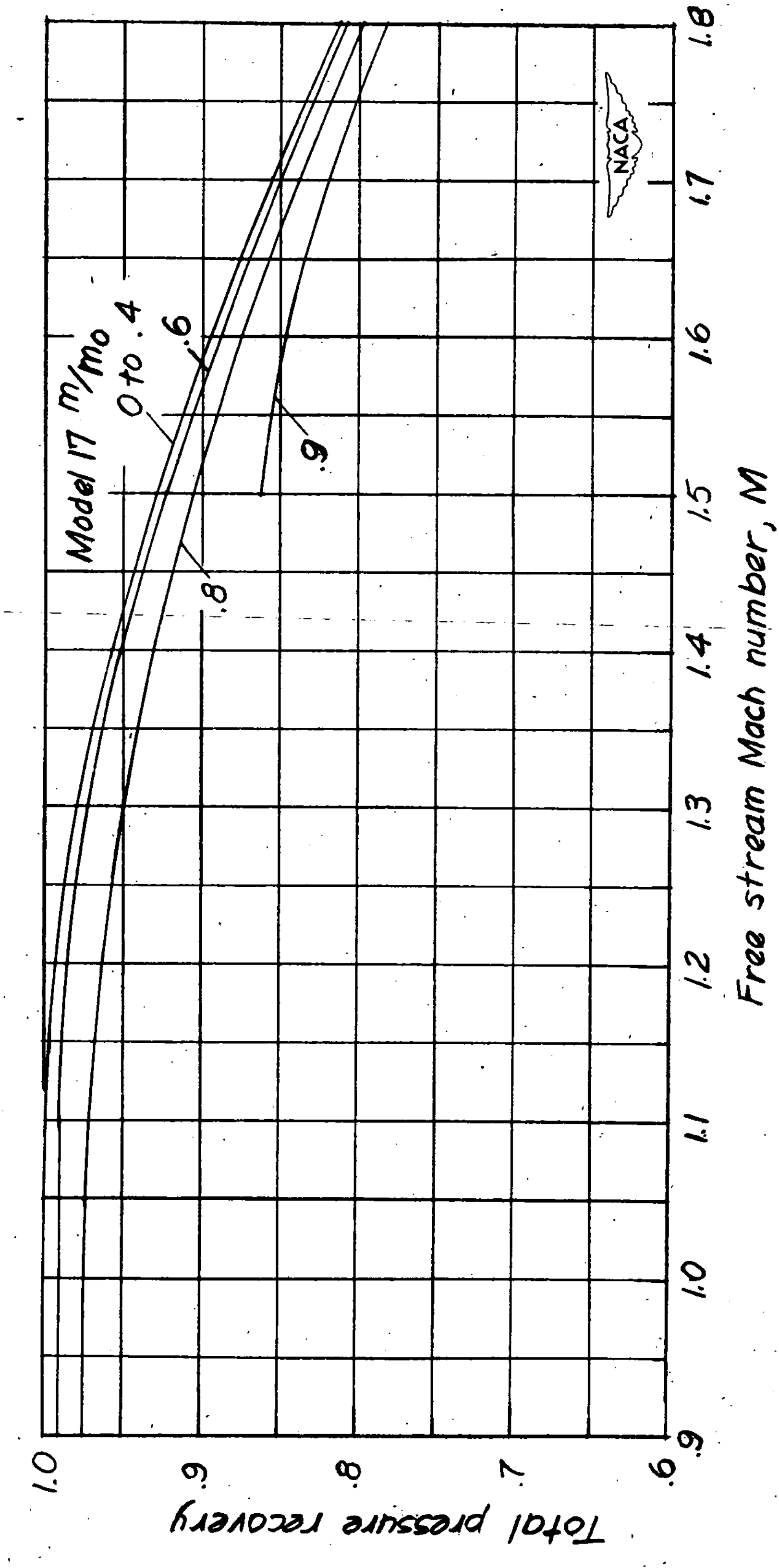

Figure 27.- Variation of total pressure recovery with Mach number for several mass-flow ratios for model 17.

[redacted]

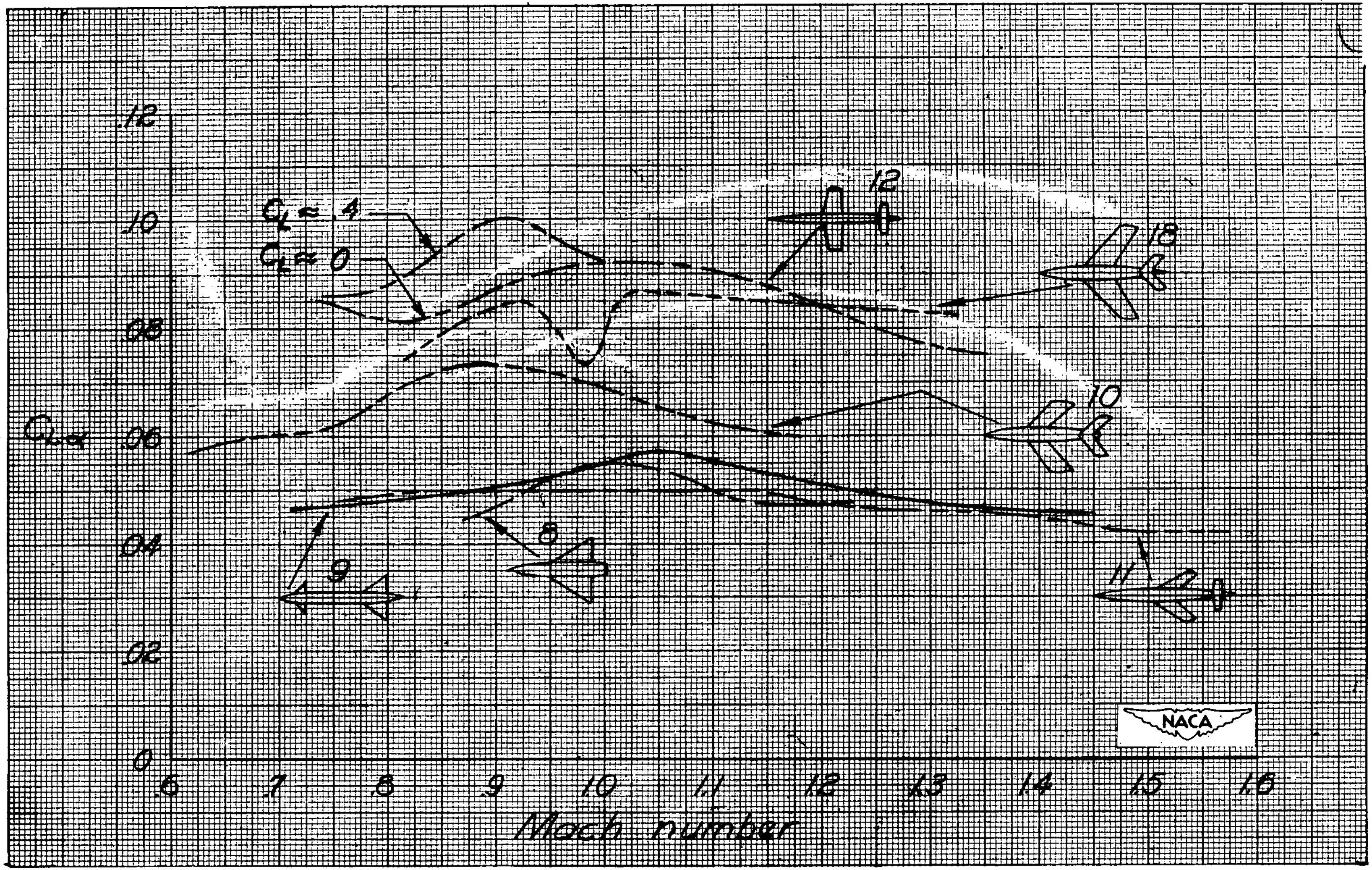

Figure 28.- Lift-curve slopes of various configurations. C_L based on total wing area to body center line.

[redacted]

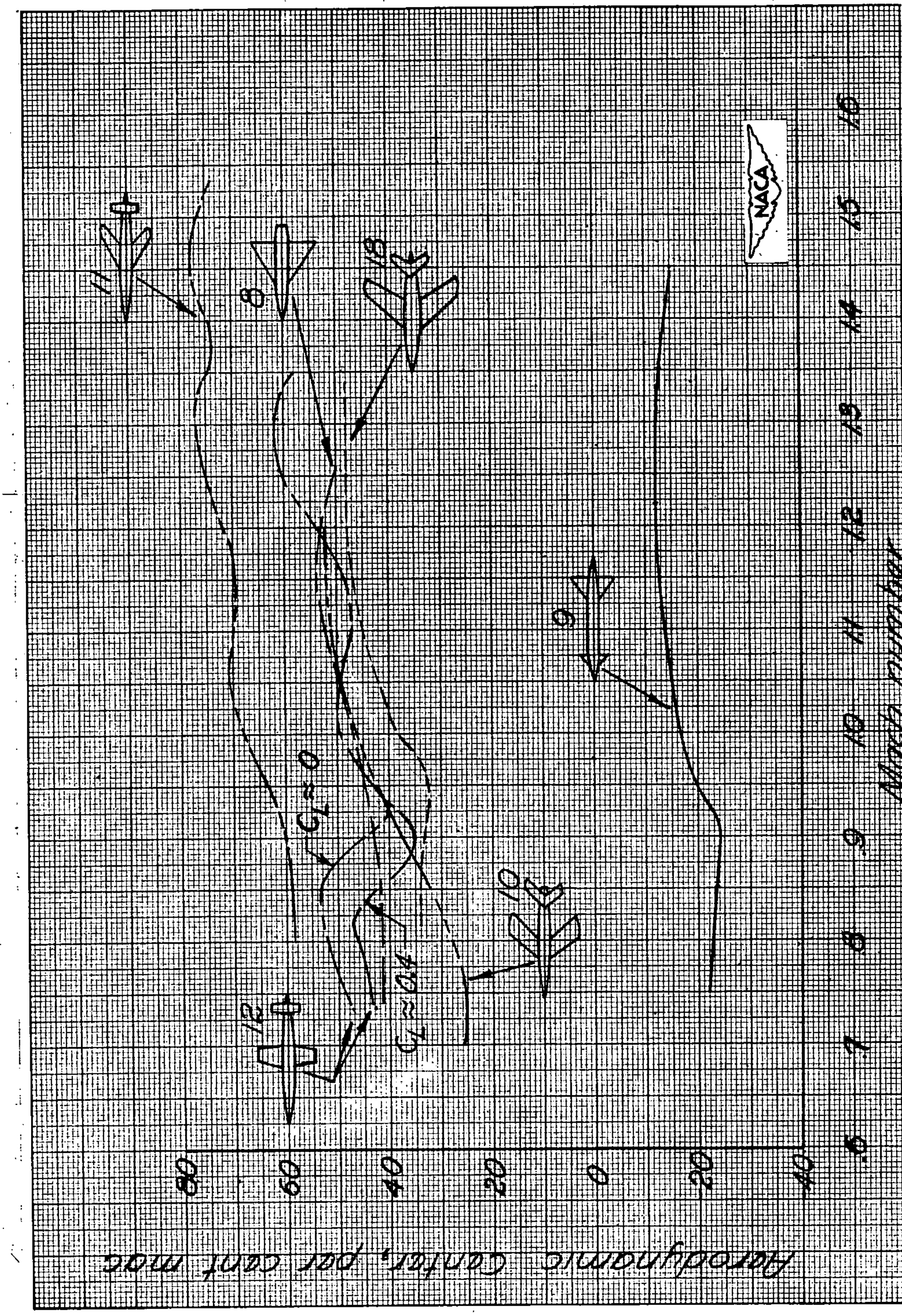

Figure 29.- Aerodynamic-center location of various configurations.

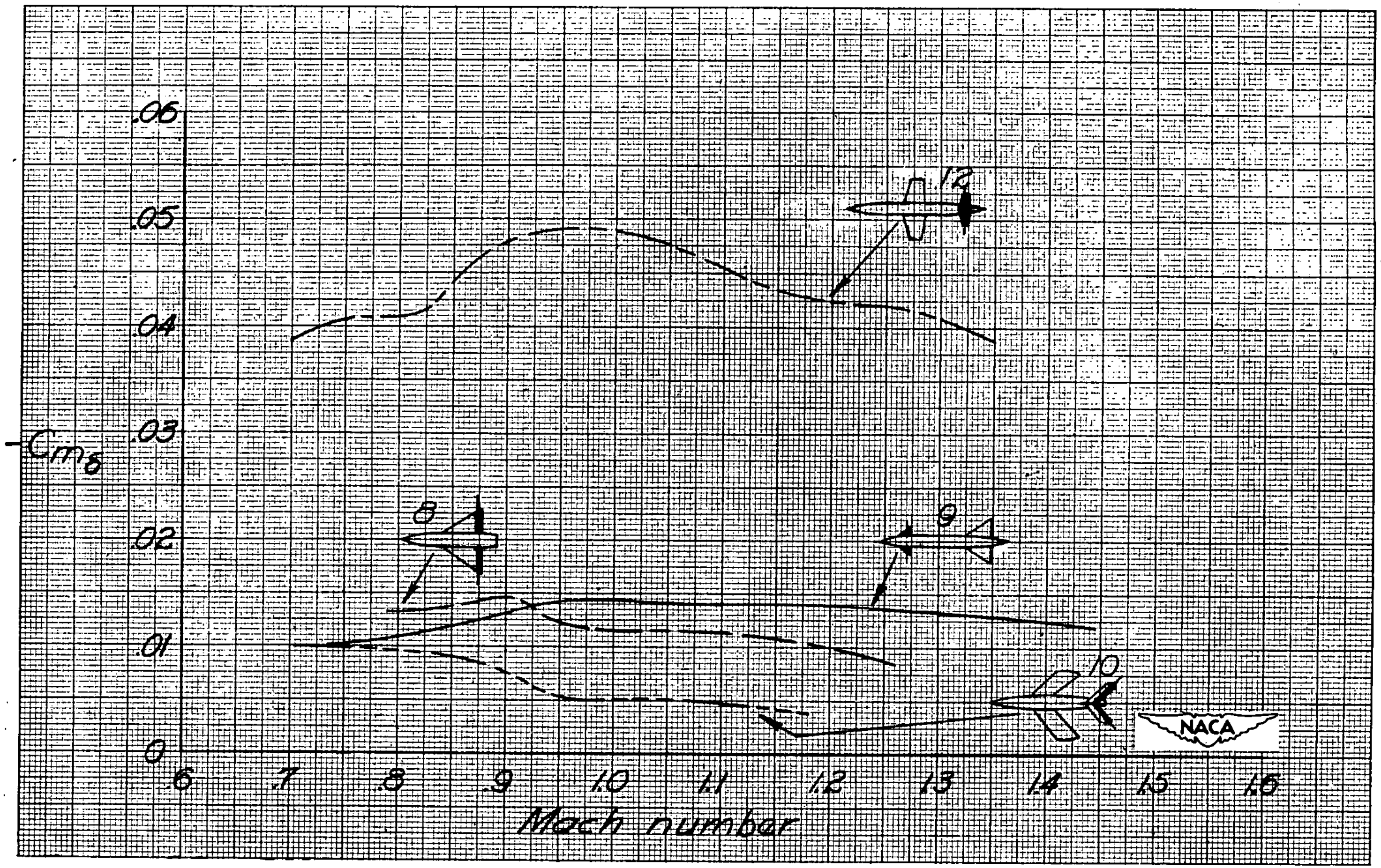

Figure 30.- Effectiveness of the longitudinal control in producing pitching moment for various configurations, based on wing dimensions to body center line.

[redacted]

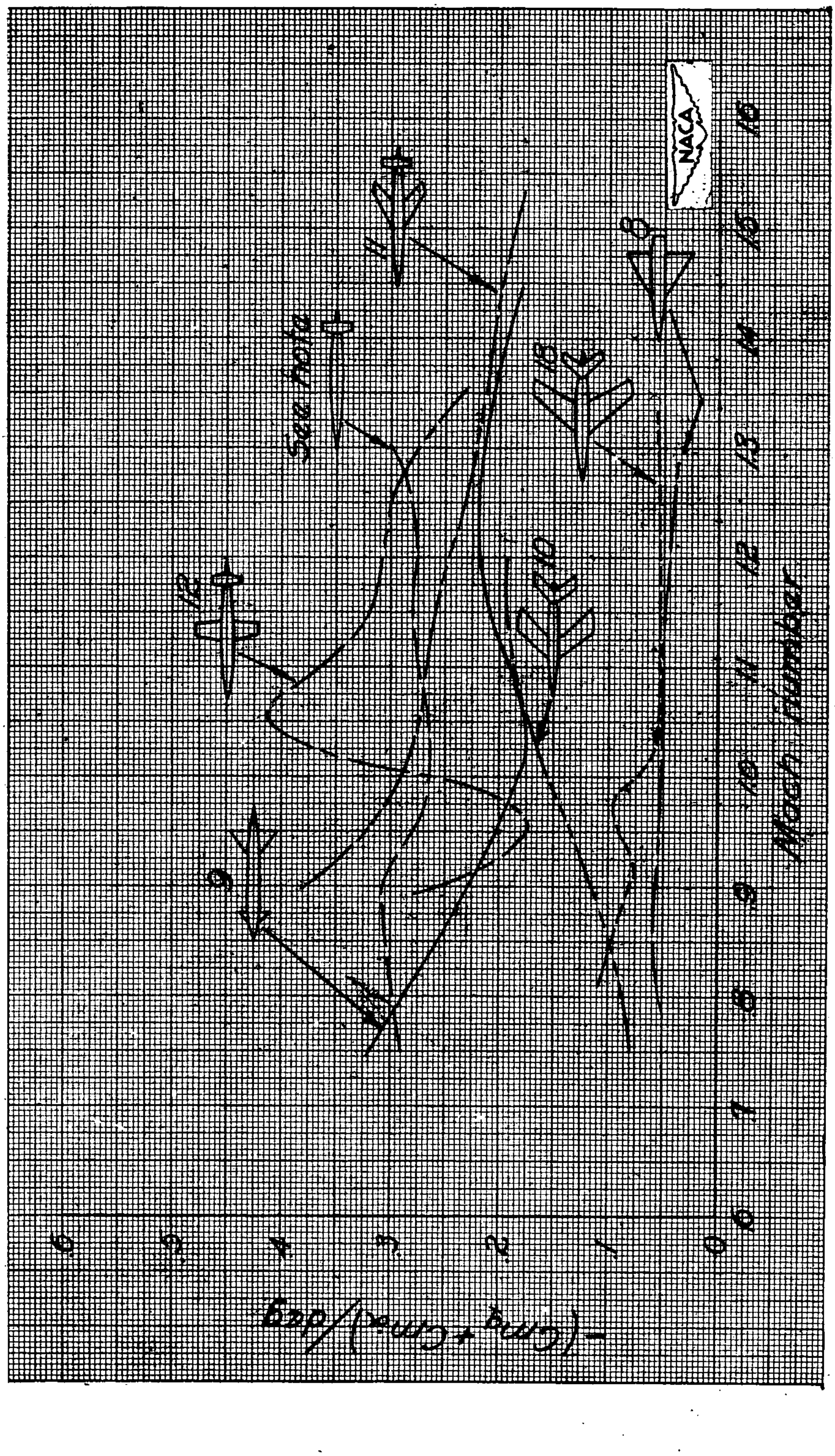

Figure 31.- Total damping-in-pitch derivative of various configurations.
Note: Data for body and tail of models 11 and 12 based on wing dimensions of model 12.

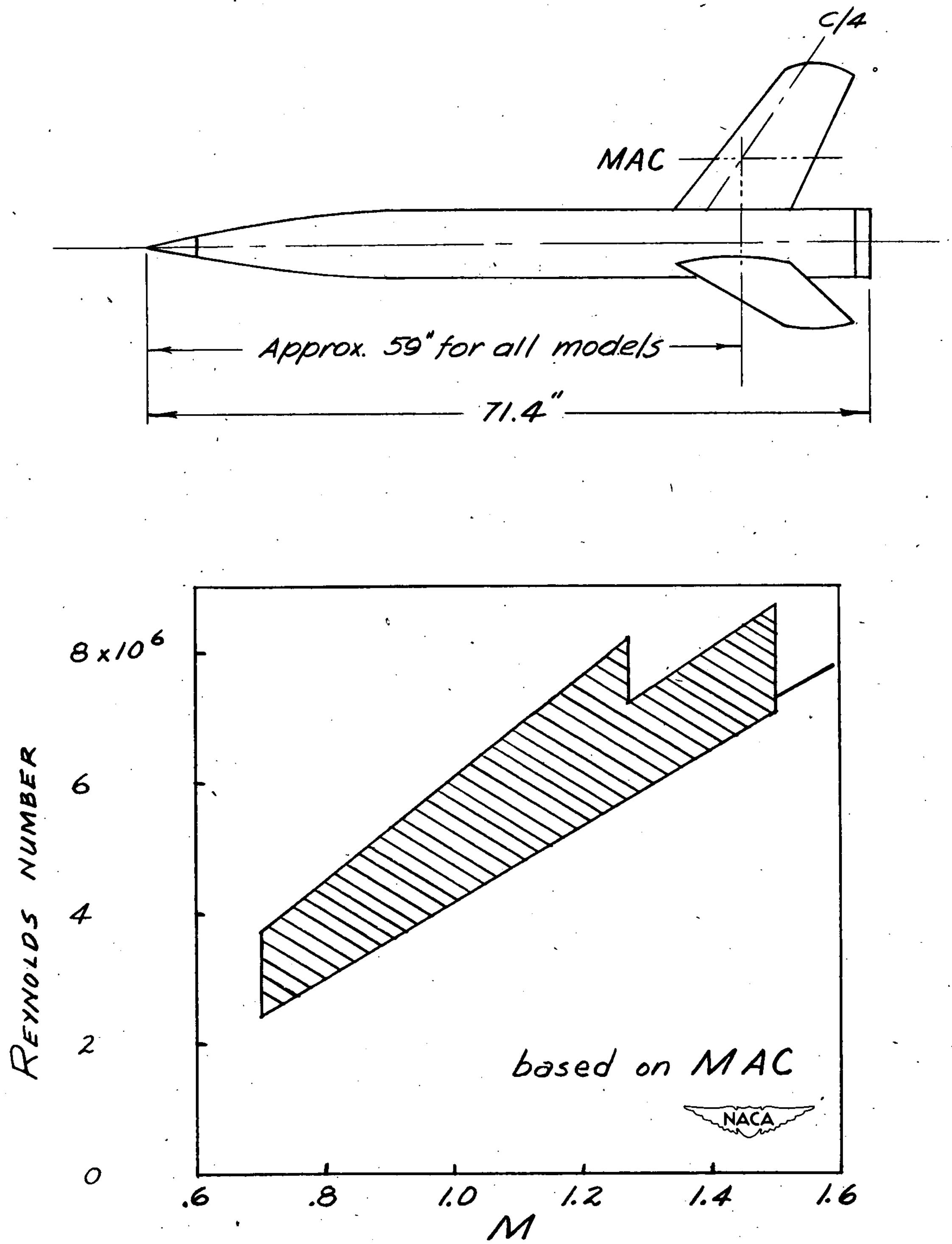

Figure 32.- Damping-in-roll model and scale of tests. Reference 11.

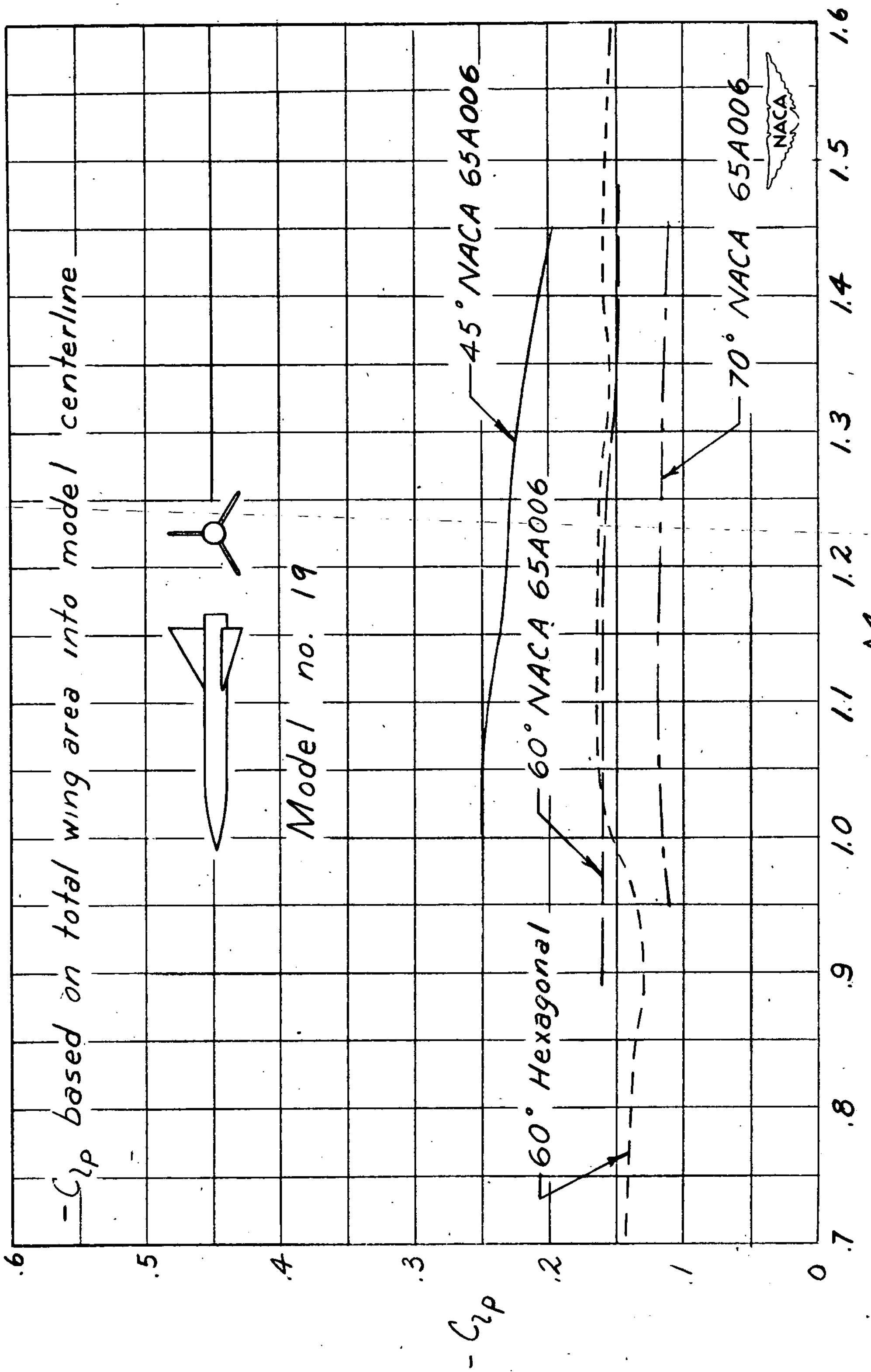

Figure 33.- Damping in roll of a series of triangular wings. Airfoil sections parallel to model center line.

[redacted]

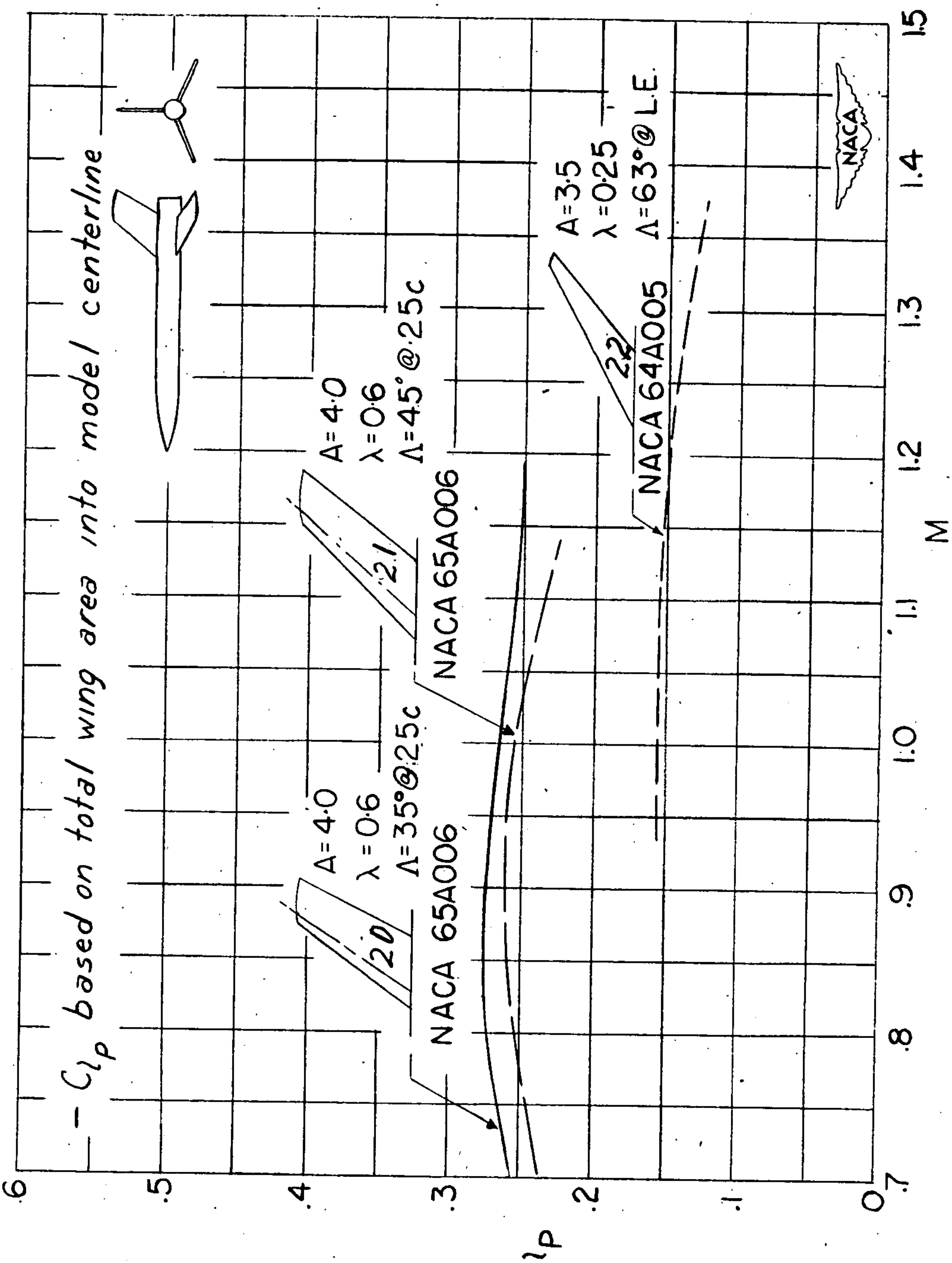

Figure 34.- Damping in roll of swept tapered wings. Airfoil sections parallel to model center line.

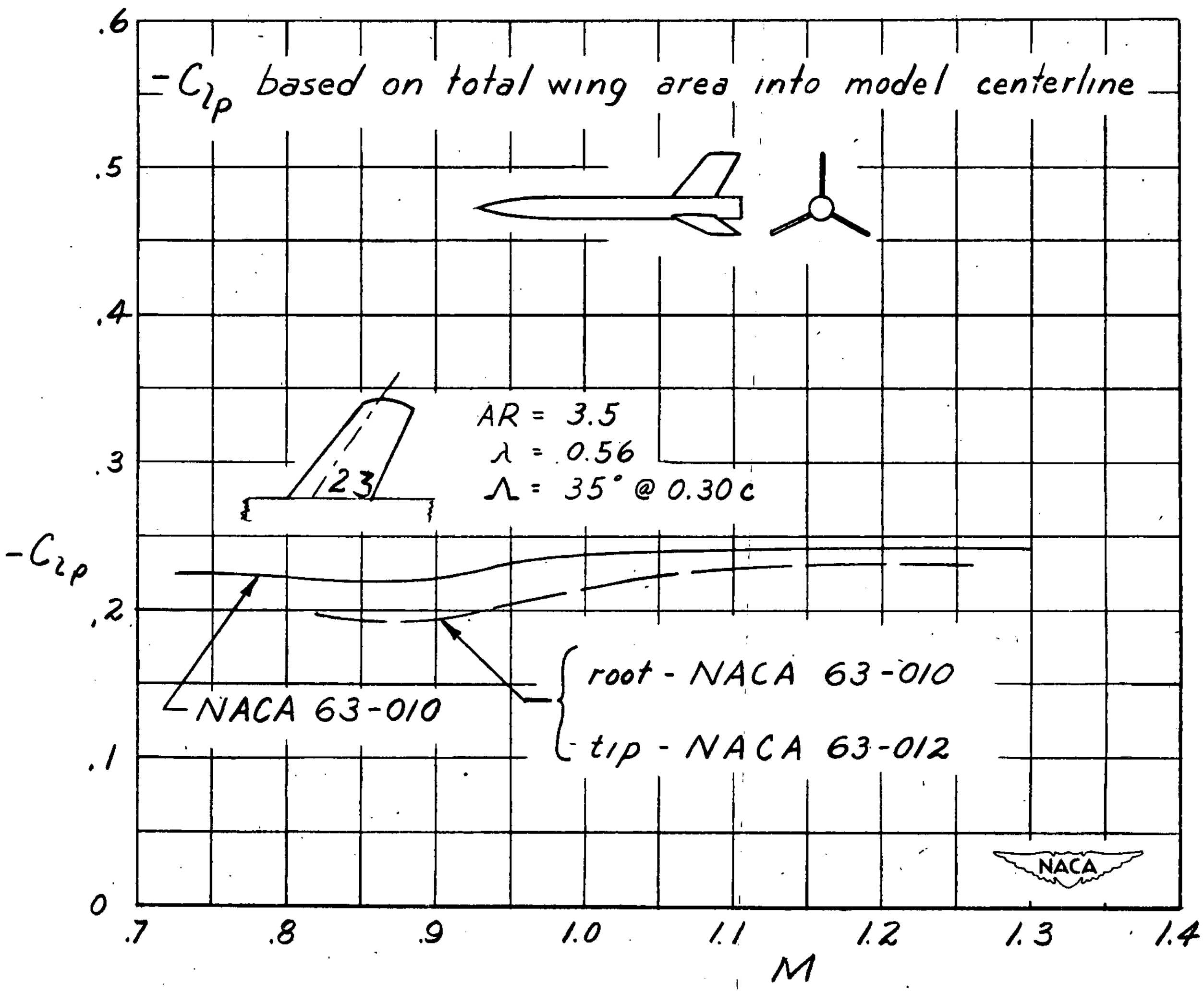

Figure 35.- Damping in roll of a swept wing with two thickness ratios. Airfoil section parallel to model center line.

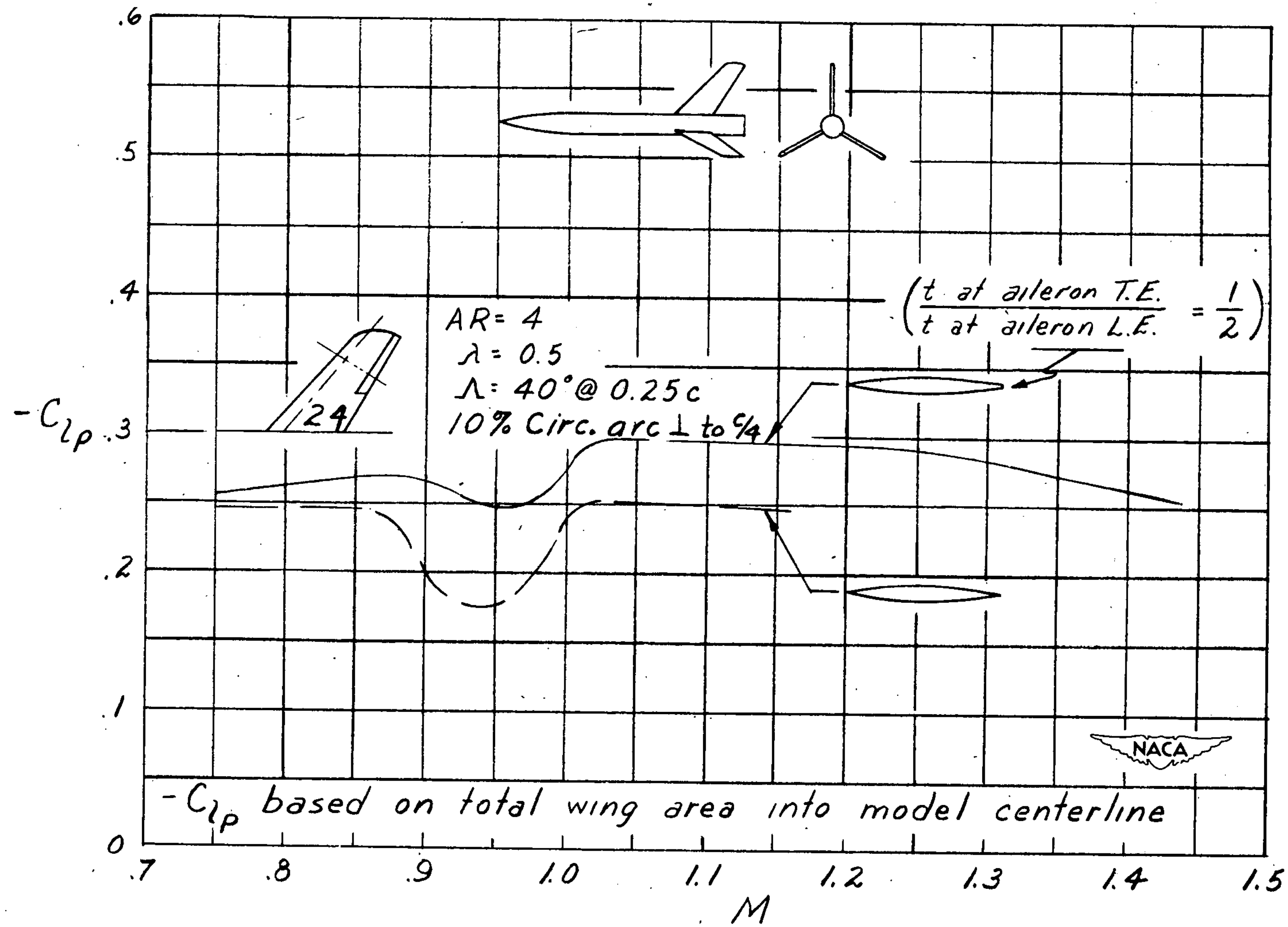

Figure 36.- Damping in roll of a swept wing with modified trailing edge.

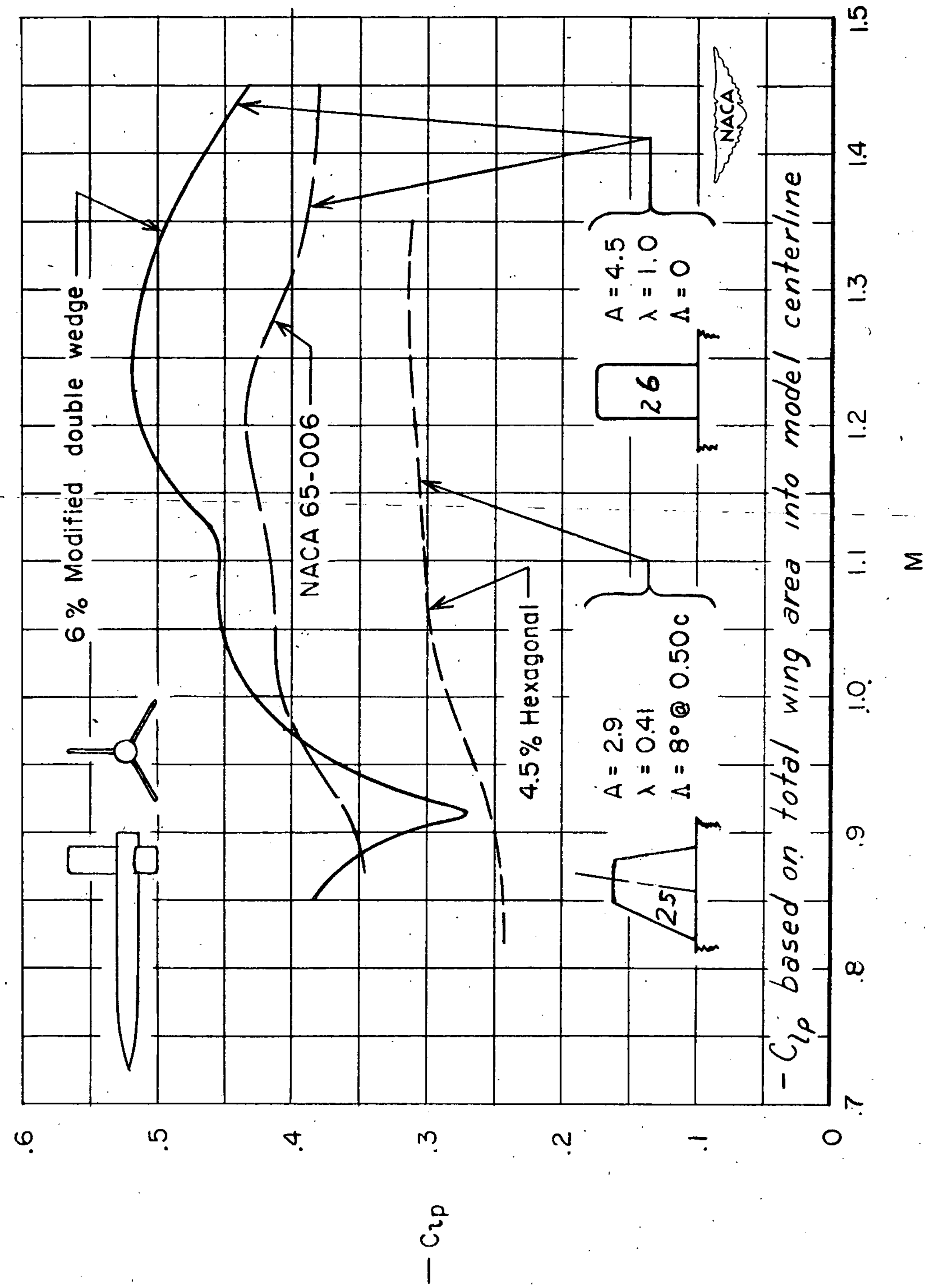

Figure 37.- Damping in roll of essentially unswept wings. Airfoil sections parallel to model center line.

[redacted]